Banff Human Organ Transplant Transcripts Correlate with Renal Allograft Pathology and Outcome: Importance of Capillaritis and Subpathologic Rejection

Ivy A. Rosales [iD],[1,2] Grace K. Mahowald,[1] Kristen Tomaszewski,[1] Kiyohiko Hotta [iD],[3] Naoya Iwahara,[3] Takuya Otsuka,[4] Takahiro Tsuji,[5] Yusuke Takada,[6] Ellen Acheampong,[1] Milagros Araujo-Medina,[1] Amy Bruce,[1] Andrea Rios,[1] Anthony Benedict Cosimi,[2] Nahel Elias [iD],[2] Tatsuo Kawai,[2] Hannah Gilligan,[7] Kassem Safa,[7] Leonardo V. Riella [iD],[2,7] Nina E. Tolkoff-Rubin,[7] Winfred W. Williams Jr.,[7] Rex Neal Smith,[1,2] and Robert B. Colvin[1,2]

Due to the number of contributing authors, the affiliations are listed at the end of this article.

ABSTRACT

Background To seek insights into the pathogenesis of chronic active antibody–mediated rejection (CAMR), we performed mRNA analysis and correlated transcripts with pathologic component scores and graft outcomes.

Methods We utilized the NanoString nCounter platform and the Banff Human Organ Transplant gene panel to quantify transcripts on 326 archived renal allograft biopsy samples. This system allowed correlation of transcripts with Banff pathology scores from the same tissue block and correlation with long-term outcomes.

Results The only pathology score that correlated with AMR pathways in CAMR was peritubular capillaritis (ptc). C4d, cg, g, v, i, t, or ci scores did not correlate. DSA-negative CAMR had lower AMR pathway scores than DSA-positive CAMR. Transcript analysis in non-CAMR biopsies yielded evidence of increased risk of later CAMR. Among 108 patients without histologic CAMR, 23 developed overt biopsy-documented CAMR within 5 years and as a group had higher AMR pathway scores ($P=3.4 \times 10^{-5}$). Random forest analysis correlated 3-year graft loss with elevated damage, innate immunity, and macrophage pathway scores in CAMR and TCMR. Graft failure in CAMR was associated with TCMR transcripts but not with AMR transcripts, and graft failure in TCMR was associated with AMR transcripts but not with TCMR transcripts.

Conclusions Peritubular capillary inflammation and DSA are the primary drivers of AMR transcript elevation. Transcripts revealed subpathological evidence of AMR, which often preceded histologic CAMR and subpathological evidence of TCMR that predicted graft loss in CAMR.

Chronic active antibody–mediated renal allograft rejection (CAMR) is characterized by transplant glomerulopathy, C4d deposition in peritubular capillaries, microvascular inflammation (mi), and circulating donor-specific HLA antibodies (DSA).[1–3] The majority of late graft dysfunction is due to CAMR,[4,5] which typically evolves subclinically over several years.[6]

CAMR has no established treatment, partly because its pathogenesis is uncertain. The microvascular endothelium is clearly the target, but three major pathways of antibody-mediated injury are possible: antibody alone, complement activation, and antibody-dependent cell-mediated cytotoxicity (ADCC).[7] A role for T cell–mediated rejection (TCMR) has been raised by appreciation of the association of previous TCMR with development of DSA and later CAMR,[6,8] and the common presence of interstitial inflammation in biopsies with CAMR.

Correspondence: Dr. Ivy A. Rosales, Massachusetts General Hospital, 55 Fruit Street, Thier 831A, Boston, MA 02114. Email: irosales@mgh.harvard.edu

Pathology studies have focused on the complement system and detection of C4d in peritubular capillaries for diagnosis.[9] However, its relevance to the pathogenesis of allograft injury has been questioned, because CAMR can occur with little or no detectable C4d deposition,[10] and C4d deposition occurs in ABO incompatible (ABOi) grafts without evidence of injury.[11] The limited efficacy of complement inhibition in clinical trials supports a complement-independent mechanism.[12–14]

The importance of microvascular inflammation in peritubular capillaries and glomeruli was proposed by observations from protocol biopsies[15] and transcript analysis[10] of renal allografts. Elegant microarray studies led by Halloran identified gene sets that were distinctive for CAMR and pointed to a role for NK cells in endothelial injury.[16,17] Finally, there is evidence that DSA alone can promote an endothelial response, without cells or complement.[18,19]

The NanoString nCounter technique permits quantitation of transcripts in formalin-fixed paraffin-embedded (FFPE) tissue, which facilitates outcome analysis from archived clinical biopsies and pathological correlations from the same tissue block used for molecular studies.[9] In this study we present the assessment of connections of the proposed mechanisms with the expression of relevant transcripts in CAMR, and the ability of transcripts to predict later CAMR or graft loss.

METHODS

Subjects

Subjects were selected on the basis of having available archival allograft biopsies with sufficient tissue remaining after diagnostic studies, with emphasis on CAMR and TCMR diagnosis. Patients received renal allografts at Massachusetts General Hospital ($n=225$), Hokkaido University Hospital (53), or Sapporo City General Hospital (48) and had biopsies in 2002–2021 ($n=326$). These included indication ($n=217$) and protocol ($n=94$) biopsies under standard immunosuppression regimens (Table 1) and living donor implantation biopsies ($n=15$). All passed quality control criteria (see below). The average time post-transplant for the biopsies was 4.0 ± 5.4 years (0.1–31 years). Repeat biopsies from 42 recipients were separated by an average of 2.1 ± 2.1 years and analyzed as separate samples.

Age, sex, time post-transplant, serum creatinine, and DSA at the time of biopsy were recorded (Supplemental Table 1). Outcomes were assessed at 3 years after biopsy, with graft failure defined as dialysis, retransplant, or serum creatinine ≥5.0 mg/dl. Outcome was censored for death with a functioning graft ($n=5$).

Pathologic Analysis

Routine FFPE biopsy blocks were retrieved. The pathologic groups were comprised of CAMR, TCMR, mixed rejection (CAMR+TCMR), no pathologic evidence of active rejection (NER), borderline/suspicious for rejection (BS), and acute

Significance Statement

Microarray analysis of renal allograft biopsies has revealed important insights, including TCMR and AMR gene sets, but is limited to specially processed samples without pathology confirmation. We used the NanoString nCounter platform to perform mRNA analysis of archived formalin-fixed paraffin-embedded kidney allograft biopsies with the Banff Human Organ Transplant Panel. We correlated Banff pathology scores in the same tissue block with validated and custom gene sets and showed the importance of capillaritis. We identified subpathological transcripts that standard pathology would not have detected and transcripts, pathology, and clinical variables that predicted graft failure in TCMR and CAMR. These findings highlight the utility of archived samples in transplant pathology research and expand our understanding of the pathogenesis of rejection.

tubular injury (ATI) (Table 1). Native kidney biopsies without light or immunofluorescence abnormalities ($n=11$) were included for comparison (control group).

Diagnoses were according to the current Banff classification.[20] Banff scores (Supplemental Table 1) were taken from the original pathology reports and confirmed on whole slide digital images (WSI, NanoZoomer, Hamamatsu) from periodic acid-Schiff–stained sections from a surface cut from the blocks used for mRNA extraction. Peritubular capillaritis (ptc), glomerulitis (g), and i-IFTA were scored on the WSI by one observer (RBC) blinded to the transcript, clinical information, and pathology report. Nine samples with no cortex on the scan were omitted from this analysis (2.7%; eight indication biopsies and one protocol biopsy).

Donor-Specific HLA Antibodies Assessment

Luminex single antigen beads assay (One Lambda, Canoga Park, CA) was performed to identify donor-specific HLA class I and II antibodies. DSA positive was defined as mean fluorescence intensity (MFI)>1000. Maximum MFI was defined as follows: $>1000–3000$, low; $3001–10,000$, moderate; $>10,000$, high; $>20,000$, very high.

NanoString RNA Assay and Quality Control Parameters

mRNA isolation was done as previously described.[21] The microtome area was cleaned with 95% ethanol and RNase AWAY (Thermo Fisher Scientific, Waltham, MA) before cutting. Five to six consecutive 20-μm curls cut from each FFPE block were immediately transferred to sterile microcentrifuge tubes and stored at room temperature. Microtome blades were then replaced, and equipment sterilized with RNase AWAY between blocks. Deparaffinization and RNA extraction were performed with the Quick-RNA FFPE Miniprep (Zymo Research, Irvine, CA). RNA concentration and purity were measured with a Nano-Drop 2000 spectrophotometer (Thermo Fisher Scientific, Waltham, MA).

Table 1. Biopsy samples

Group		N
Transplant biopsies		
Acute tubular injury (ATI)		16
NER		85
BS		33
TCMR		49
TCMR1	26	
TCMR2	23	
CAMR		120
CAMR	95	
CAMR + TCMR	25	
ABOi C4d$^+$		8
Donor biopsies, living (donor)		15
Total transplant biopsies		326
Native kidney, normal histology (control)		11
Total biopsies		337

Gene expression of the FFPE tissue–derived RNA isolates was quantified using the nCounter MAX System (NanoString Technologies, Seattle, WA). The Banff Human Organ Transplant (B-HOT) 770-gene panel, selected primarily from published microarray studies of allografts, was used for hybridization (NanoString Technologies).[9] The major limitation is that the gene set is predefined and less suited for discovery studies.

Quality Control

Quality control assessment and normalization were performed with nSolver Software 4.0 (NanoString Technologies) using the recommended default parameters for quality control flagging for RNA content, imaging, and positive controls. The acceptable binding density threshold was increased from <2.25 to <3.26 probes per μm^2, which had little or no effect on the transcript results. Each sample was first normalized to the geometric mean of the positive controls (with default flagging of normalization factors <0.3 and >3), followed by normalization to the geometric mean of the 12 housekeeping genes (with default flagging of normalization factors <0.1 and >10). All samples used in this analysis passed these quality control parameters. Five samples had low RNA retrieval and were not used (1.5%), all protocol biopsies.

The NanoString B-HOT panel DNA standard, which has targets for each of the test probes, was run three times over 2 months to test technical reproducibility of the instrument. The Pearson correlation coefficient (r) between each run was 0.999 for the 758 genes in the panel. To test for preparation and biologic reproducibility, repeat assays were carried out on four samples. Pathway scores between the same blocks had r values of 0.980 and 0.986; between different cores from the same biopsy the r values were 0.887 and 0.922. The average storage time of the blocks was 6.9±4.7 years (0.1–18.1 years). The slow decline in RNA yield by storage time was fully corrected by software normalization with housekeeping genes (Supplemental Figure 1).

Data Analyses

The NanoString Advanced Analysis software 2.0 was used for differential gene expression and pathway analysis. Pathways were chosen from relevant gene sets defined in microarray studies,[9,22–25] published cellular pathways,[9] and custom pathways (Supplemental Table 2). The pathway score is equal to the first principal component of the gene set.[26] Principal component (PC) analysis scores use a linear combination (a weighted average) of its gene expression values, weighing specific genes to capture the greatest possible variability in the data.[26] All pathway and cell type gene sets are available in the supplementary Excel file (Supplemental Table 2). Groups were compared by Kruskal–Wallis with multiple pairwise comparisons using the Steel–Dwass–Critchlow–Fligner procedure, ordinal logistic regression, t tests, chi square, Fisher's exact, Mann–Whitney statistics, ANOVA, and MANOVA (XLSTAT, New York, NY; GraphPad Prism, San Diego CA; JMP 16, Cary, NC). Differential gene expression was corrected for multiple comparisons with the Benjamini-Yekutieli (B-Y method).

Random forest (RF) classification (XLSTAT) was used to test all variables (clinical, pathologic, pathway or cell type, and individual transcripts; $n=953$) for their strength to predict graft failure in 3 years in CAMR/Mixed and BS-TCMR groups. Trees ($n=2000$) were generated with random samples of approximately 70% of patients. The patients left out were classified on each random tree (bootstrap or "bagging") to yield the majority classification. The importance of each variable was ranked and the top 3%–4% were tested to see whether the RF classification improved the predictive power of the pathologic diagnosis alone. Repeated RF (10×) was used to select the 70%–80% commonly identified (3%) variables, and those were repeated 10× to yield the most common classification of outcome (Supplemental Table 3).

RESULTS

Validated Gene Sets Distinguished Chronic Active Antibody–Mediated Rejection and T Cell–Mediated Rejection from Other Diagnoses

The B-HOT panel distinguished histologic CAMR or TCMR in aggregate using AMR and TCMR gene sets or pathways that were discovered and validated in microarray studies. Representative results are given for DSAST[17] and TCMR[26] (Figure 1). TCMR and CAMR were distinguishable even when stratified by time post-transplant or by first biopsies only (data not shown).

Correlations of Pathway Scores with Banff Scores and Donor-Specific HLA Antibodies Levels

An advantage of nCounter assays is the ability to compare the pathology and transcripts from the same tissue block. We postulated that pathogenic insights might best be revealed by determining which individual Banff lesions correlated with
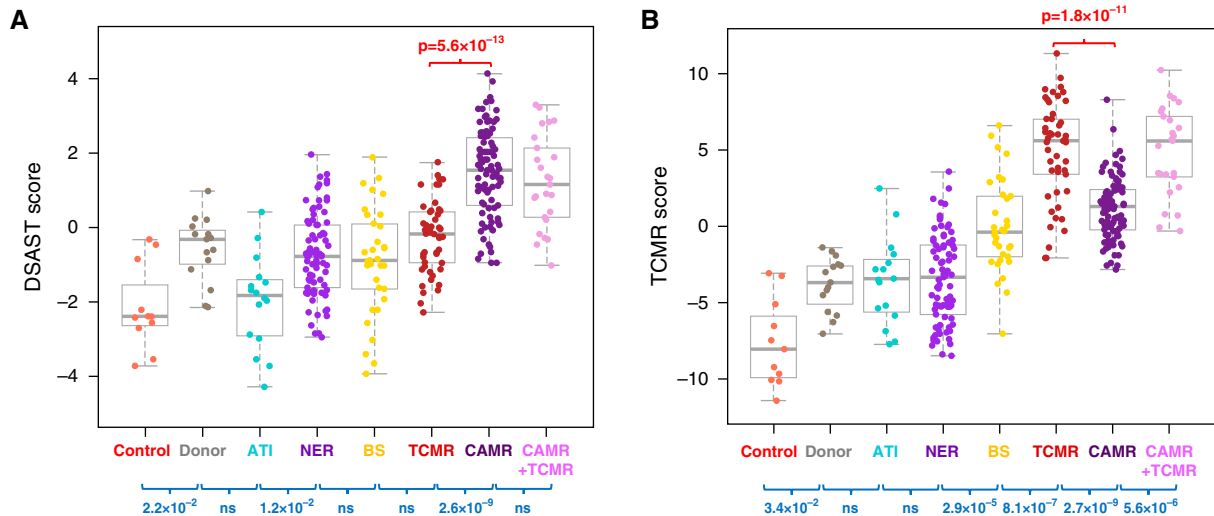
Figure 1. DSAST and TCMR pathways distinguish CAMR from TCMR and other diagnoses. (A) This box and whisker plot shows the DSAST pathway score for each pathologic category. The discrimination between CAMR and TCMR is highly significant in aggregate. The presence of TCMR does not affect the DSAST score in CAMR. A minority of TCMR, BS, and NER scores are high, and similar to CAMR. These patients include a substantial fraction that subsequently developed overt CAMR (Figure 8). (B) The TCMR pathway shows strong discrimination between TCMR and CAMR and between CAMR and mixed (CAMR+TCMR). TCMR pathway scores also discriminate between BS and NER and between TCMR and BS (P values by Kruskal–Wallis test, blue; Mann–Whitney test, red).

elevation of AMR pathway scores, including DSAST,[17] ENDAT,[10] AMR,[27] and CAMR-NHP.[28] The results were similar for these AMR pathways and representative data are shown. CAMR and mixed rejection (CAMR+TCMR) are combined unless noted; the conclusions are similar when CAMR is analyzed alone (data not shown).

Interstitial Inflammation and Tubulitis

Although interstitial inflammation (i) and tubulitis (t) are not criteria for CAMR, they are often present, and may reach the level diagnostic of TCMR. AMR pathway scores in CAMR samples were not affected by interstitial inflammation (Figure 2A) or tubulitis (Supplemental Figure 2A). TCMR pathway scores increased with increased interstitial inflammation and tubulitis in all samples including CAMR, as expected[29] (Figure 2B, Supplemental Figure 2B). Patients with CAMR and TCMR with similar Banff i and t scores had similar TCMR pathway scores. Thus, interstitial inflammation and tubulitis are not responsible for increased levels of AMR pathway transcripts but reflect a variable component of TCMR.

C4d Deposition

C4d deposition is recognized as a common, but not invariable, diagnostic feature of CAMR. The relevance of C4d to AMR transcripts was determined by comparing the AMR pathway scores with C4d deposition in peritubular capillaries. C4d extent had no effect on AMR pathway scores in CAMR (Figure 3A). AMR pathway scores were increased significantly even in C4d0 CAMR biopsies compared with biopsies with no evidence of rejection ($P=2.6\times10^{-17}$). This indicates that something other than C4d deposition

influences expression of AMR transcripts. Mixed rejection (CAMR+TCMR) had a higher frequency of C4d2–3 (88%) than CAMR alone (46%, $P=1.7\times10^{-4}$ chi square).

To test further the contribution of C4d, we compared protocol biopsies from C4d$^+$ ABOi allografts with protocol biopsies from ABO compatible allografts that had NER (C4d0, g0, and ptc0). No significant differences were detected in AMR pathway scores (Figure 3B) or individual transcripts. Protocol C4d$^+$ ABO compatible allografts had elevation of AMR pathway scores equivalent to indication biopsies with CAMR.

Microvascular Inflammation (Banff Glomerulitis and Peritubular Capillaritis)

A second criterion for CAMR is mi, g+ptc) in glomeruli and peritubular capillaries. The ptc score showed strong correlation with AMR pathway scores (Figure 4A) and NK cell and Endothelium pathway scores (Figure 4, B and C). CAMR ptc0 (CAMR with peritubular capillary inflammation below Banff threshold) had higher AMR pathway scores than NER ptc0 ($P=3.7\times10^{-6}$); most of these were DSA$^+$ patients (92%). CAMR ptc0 also had higher NK and Endothelium pathway scores than NER ptc0 (Figure 4, B and C). The g score did not correlate with the DSAST pathway (Supplemental Figure 3A) and had a weak correlation with the AMR pathway[27] ($r=0.194$, $P=3.4\times10^{-2}$). The i and g scores correlated with ptc scores in CAMR/Mixed ($P=3.0\times10^{-4}$ and 2.6×10^{-2}, respectively). The i scores did not correlate with ptc scores in the NER and BS-TCMR groups ($P>0.05$).
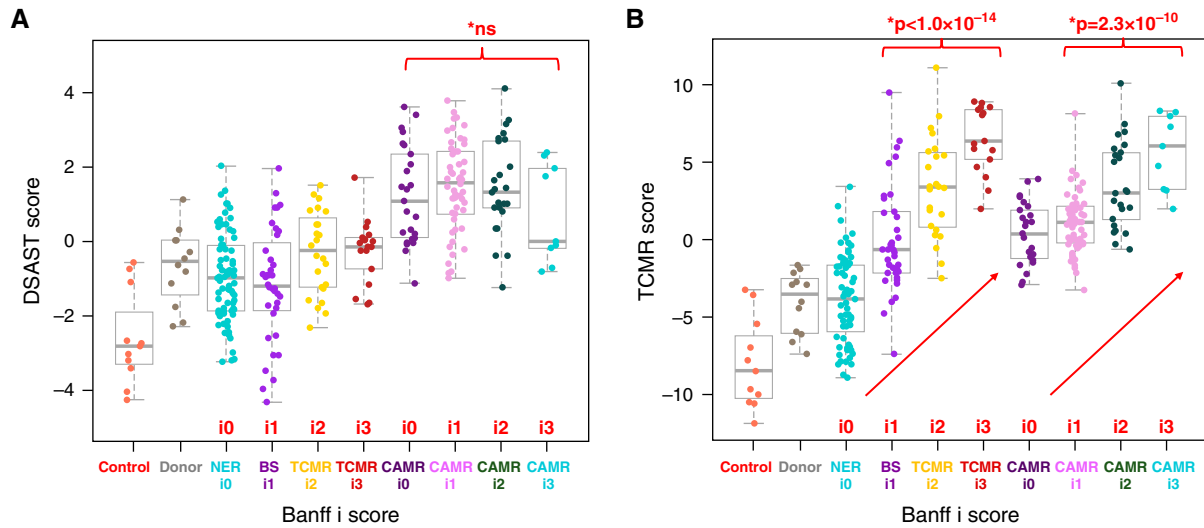
Figure 2. AMR pathway transcripts are not affected by interstitial inflammation in CAMR, whereas TCMR pathway transcripts correlate with interstitial inflammation. Interstitial inflammation (Banff i scores) for BS and TCMR do not affect the AMR pathway score (A) but correlate strongly with TCMR pathway scores (B). (A) Shown is a representative AMR pathway, DSAST. A moderate increase in DSAST pathway scores is correlated with Banff i2–3 scores in TCMR samples. This might indicate a component of AMR not detected histologically in these patients, or a direct effect of the infiltrate on the AMR pathway transcripts independent of AMR. However, the DSAST pathway scores are not different between NER with Banff i0 and BS with Banff i1 or between TCMR Banff i2 and TCMR Banff i3. Similar results are seen with tubulitis (Banff t scores; Supplemental Figure 2). CAMR group includes mixed (CAMR+TCMR). Similar correlation was seen in CAMR alone (not shown) (*P* values by logistic regression, red).
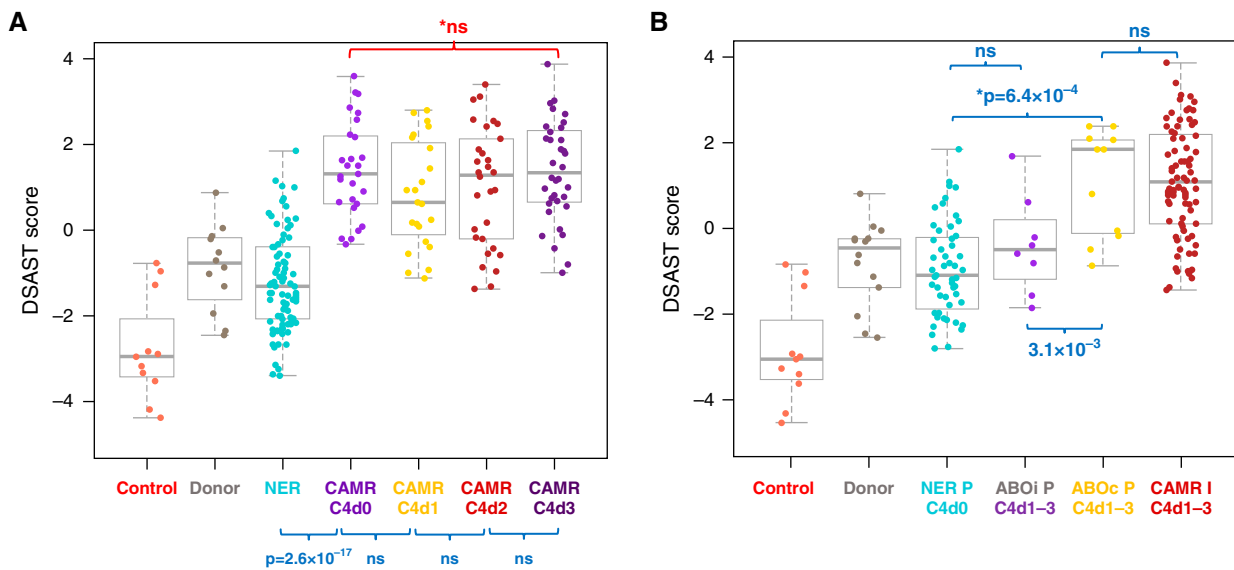

Figure 3. AMR transcripts are not affected by complement (C4d) deposition. ABOi C4d$^+$ grafts with no evidence of rejection show no significant increase in AMR pathway scores. (A) The DSAST pathway score is plotted against extent of C4d deposition (Banff C4d score). There is no correlation of extent of C4d deposition on AMR pathway scores in CAMR (with or without TCMR). AMR pathway scores increased independent of C4d deposition from biopsies with NER to biopsies of C4d-negative CAMR ($P < 2.6 \times 10^{-17}$). (B) AMR pathway scores of ABOi C4d$^+$ protocol biopsies are similar to protocol biopsies from C4d ABO compatible (ABOc) grafts with NER. ABOi grafts typically have no mi, although the ABOi graft with the highest score had ptc1. ABOc C4d$^+$ protocol biopsies have AMR pathway scores >NER C4D0 and equal to CAMR indication biopsies (*P* values by Kruskal–Wallis test, blue; Mann–Whitney test, red. I, indication biopsy; P, protocol biopsy).
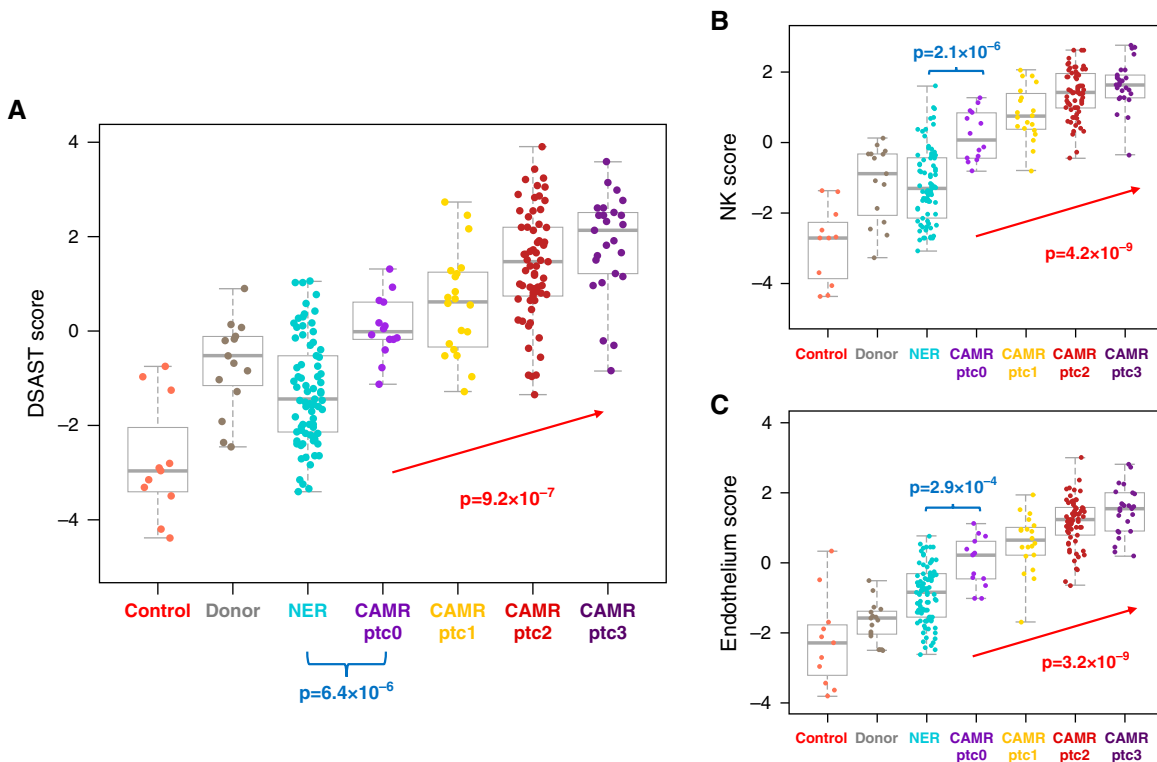
Figure 4. In CAMR, peritubular capillaritis (Banff ptc) scores correlate with AMR, NK cell, and Endothelium pathway scores. (A) DSAST pathway scores correlate with Banff ptc scores in CAMR. (B) and (C) NK (*CCL4, CD160, FCGR3A/B, FGFBP2, GNLY, KLRD1, KLRF1, MYBL1, NKG7, PRF1, SH2D1B, TRDV3*) and Endothelium (*ACKR1, CAV1, MALL1, PECAM1, PLA1A, PLK2,* and *VCAN*) pathway scores also correlate with ptc scores (*P* values by logistic regression, red; Mann–Whitney test, blue).

Other Correlations

Transplant glomerulopathy (cg) scores, a pathologic feature of chronicity in CAMR, did not correlate with AMR or TCMR pathways (Figure 5A, Supplemental Figure 3B). The NK pathway correlated negatively with cg scores ($r=-0.286$, $P=1.6 \times 10^{-3}$). A custom gene set on the basis of specific glomerular endothelial genes (*EHD3/SOST*)[30,31] decreased with increasing cg scores (Figure 5B). The cg score also correlated with g but not ptc scores (Figures 5, C and D). The %i-IFTA score correlated best with two pathways: Extracellular matrix organization ($P=8.4 \times 10^{-6}$) and Progression GoCAR ($P=2.6 \times 10^{-6}$).[32,33]

AMR pathway scores were not affected by v lesions in patients with TCMR and CAMR (Supplemental Figure 4A). TCMR scores were higher in samples with v lesions from both TCMR and mixed-rejection biopsies (Supplemental Figure 4B). Other Banff scores did not correlate with AMR pathway scores (ci, ct, cv, ah, i-IFTA).

Donor-Specific HLA Antibodies

Most patients with CAMR had detectable DSA (88%; 99 out of 112). Four patients who were DSA⁻ were C4d-negative, but had mi scores of 3,4,5,6 and cg scores of 1,3,3,3 (Banff "Suspicious"). DSA⁺ CAMR had higher AMR pathway scores than DSA⁻ CAMR (Figure 6A).

DSA⁺ CAMR showed increasing AMR pathway scores with increasing levels of DSA (Figure 6B); DSA⁻ and DSA low groups were similar. Other AMR pathways also had modest correlation with DSA⁺ versus DSA⁻ (ENDAT $P=7.7 \times 10^{-3}$, AMR $P=3.5 \times 10^{-2}$). DSA⁺ CAMR had increased expression of six individual genes: *KIR3DL1* (NK cells), *CXCL12*, and four endothelial genes, *HSPA12B, MMRN2, CD34, S1PR1* (Supplemental Figure 5). DSA⁺ CAMR also had more extensive C4d deposition than DSA⁻ CAMR (35.1±34.3% versus 9.7±14.8%, respectively; $P<0.02$). Serum creatinine at biopsy, mi, and years post-transplant were not different (data not shown).

Prediction of Later Chronic Active Antibody–Mediated Rejection by Transcripts

Although AMR pathways distinguished CAMR from other diagnoses in aggregate with high probability, individual patients with non-CAMR diagnoses overlapped with the levels in CAMR biopsies. We sought evidence whether these overlapping patients have CAMR below the threshold of pathology criteria. We analyzed patients who had been followed for ≥3 years after a biopsy showing NER, BS, or TCMR for the subsequent occurrence of biopsy-confirmed CAMR. Of 64 patients with NER on biopsy, 12 (18.8%) developed CAMR, as did 16 (36.4%) of 44 patients with
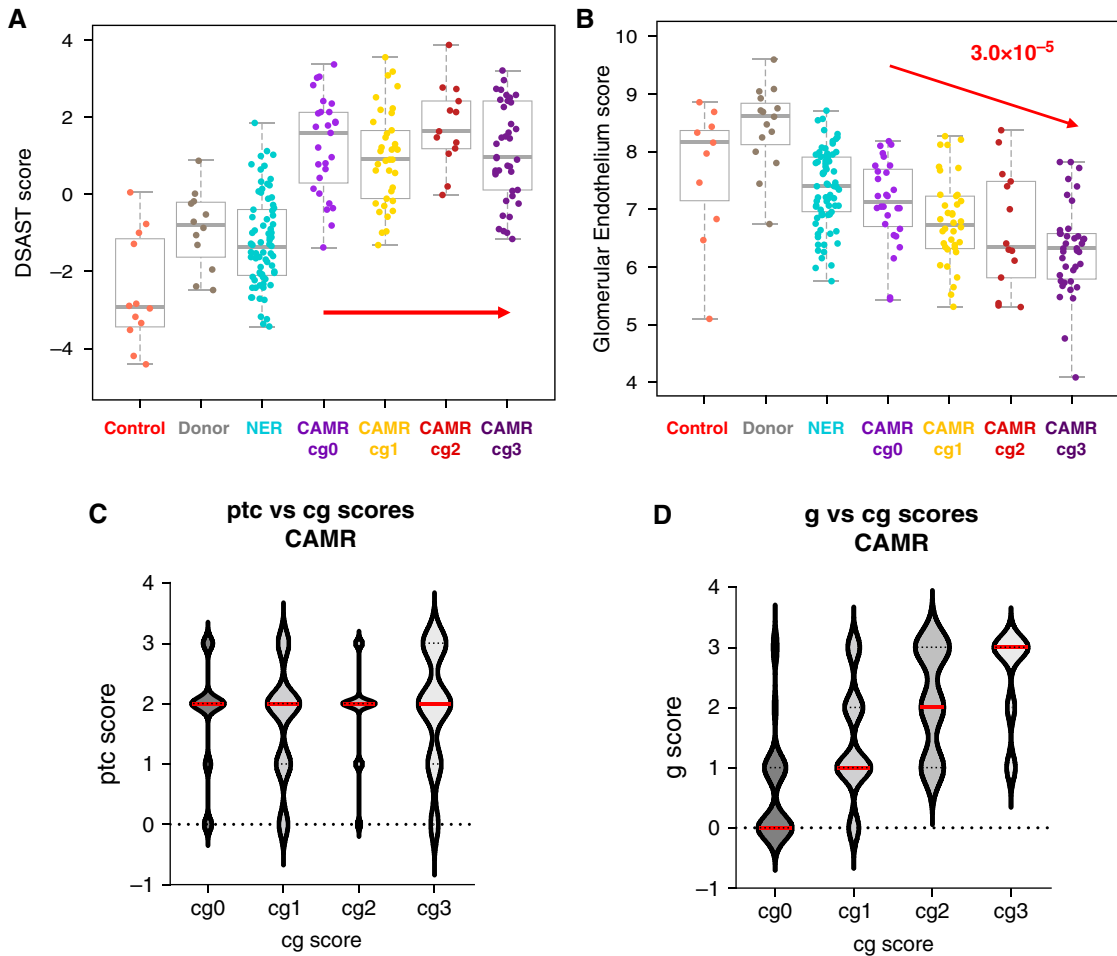
Figure 5. In CAMR, transplant glomerulopathy (Banff cg) scores do not correlate with AMR pathway scores but correlate with glomerular Endothelium scores. Transplant glomerulopathy (Banff cg) scores correlate with glomerulitis (Banff g) scores. (A) DSAST pathway scores show no correlation with transplant glomerulopathy (Banff cg) in CAMR. (B) Glomerular endothelium scores (*EHD3, SOST*) scores correlate severity of transplant glomerulopathy. (C) and (D) Transplant glomerulopathy scores do not correlate with peritubular capillary i (Banff ptc) but glomerulitis scores (Banff g) do (*P* values by logistic correlation, red; Mann–Whitney test, blue).

BS-TCMR, together termed "PreCAMR" biopsies. The AMR pathway scores were higher in PreCAMR biopsies from patients that developed CAMR within 5 years compared with those that did not ($P=1.2 \times 10^{-5}$). Patients who developed CAMR >5 years later had no elevation in AMR pathway scores in the PreCAMR biopsy (Figures 7A, Supplemental Figure 9). The most discriminating gene set among the AMR pathways was a 10-gene set previously associated with DSA (DSA10)[34] (Figure 7B). Of those with DSA10 values above zero, 51% of patients developed CAMR within 5 years, compared with 14% of those with pathway scores below 0 ($P=1.3 \times 10^{-6}$, chi square, Figure 7B). Therefore, a substantial portion of the overlap is not due to false positives, but rather to "subliminal" AMR unappreciated by standard pathology. The fraction of those that developed CAMR within 5 years and DSA$^+$ at the time of the biopsy (33%, 5/15) is higher but not statistically

distinguishable from the 10% (three out of 29) that did not develop CAMR ($P=0.14$, chi square). AMR transcript levels were similarly elevated in DSA$^-$ and DSA$^+$ PreCAMR groups (data not shown). All with CAMR >5 years later were DSA$^-$ at the time of biopsy.

A univariate analysis of all parameters (clinical/laboratory, pathology, and transcript pathways) revealed four variables significantly different in the PreCAMR group at a threshold of $P<0.05$ (i, t, mi, and DSA10; $P=0.01$, 0.03, 0.04, and 1.2×10^{-5}, respectively; Supplemental Table 4). Standard least-squares regression against DSA10 showed there were no significant interactions between PreCAMR and mi, i, or t. MANOVA only showed significance for DSA10. An RF classifier with ten-fold validation showed the proportional contributions for PreCAMR were 0.56 (DSA10), 0.26 (t), 0.18 (i), and 0.01 (mi). We conclude that DSA10 is the dominant predictor of later CAMR.
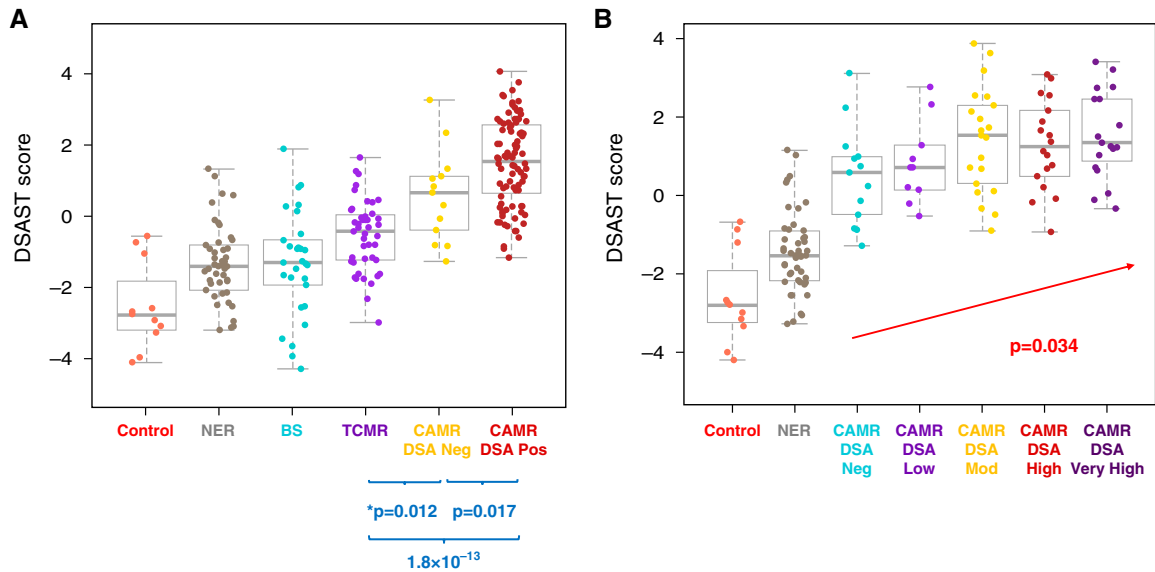
Figure 6. AMR pathway scores are higher in DSA$^+$ CAMR and correlate with DSA maximum MFI. (A) DSAST pathway scores are significantly higher in DSA$^+$ CAMR than DSA$^-$ CAMR. DSA$^-$ CAMR is also higher than TCMR. (B) AMR pathway scores correlate with DSA maximum MFI (*P* values by Mann–Whitney test, blue; logistic regression, red).

Outcome

The use of archived FFPE samples and the nCounter assay facilitates correlation of transcripts with long-term outcome. Indication biopsies were analyzed for outcome, because graft loss was rare within 3 years of a protocol biopsy ($n=1$ of 81). Graft loss within 3 years after CAMR, mixed-rejection (CAMR+TCMR), or BS-TCMR (Borderline+TCMR) biopsies was 36%, 75%, and 24%, respectively (all pairs, $P<0.005$ except CAMR versus TCMR, $P=0.16$).

CAMR/Mixed-rejection graft loss was associated with a higher serum creatinine at biopsy, C4d, i, %i-IFTA, and v scores and fibrosis (Table 2). In the TCMR group, only mi (g+ptc) scores and DSA correlated with later graft loss (Table 2). The top transcript pathways associated with graft loss in both CAMR and TCMR groups were damage and innate immunity pathways, including macrophage transcripts (Figure 8, Supplemental Figure 7). Higher AMR
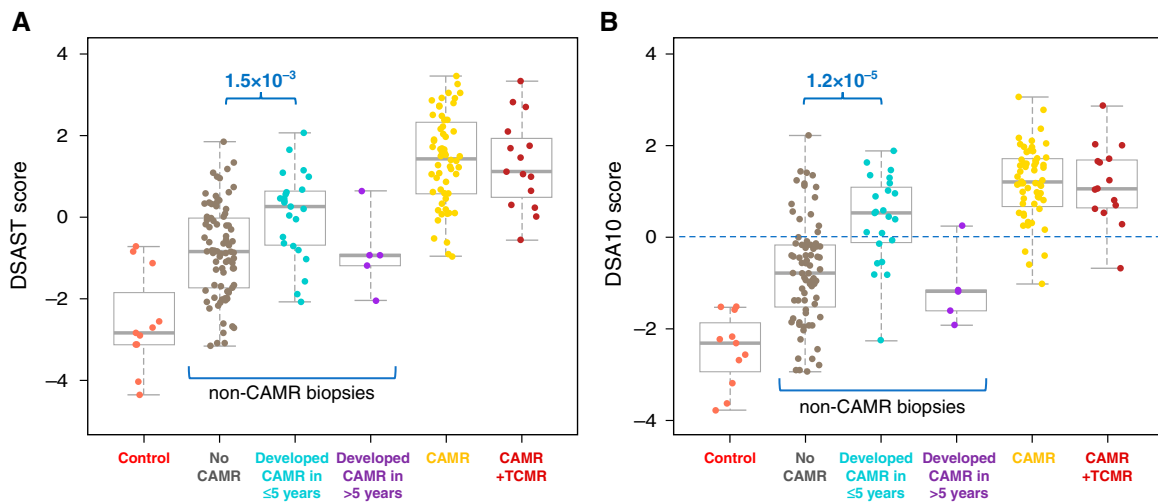
Figure 7. Pathways that predict CAMR within 5 years of biopsy. (A) AMR pathway scores are higher in non-CAMR biopsies from patients that later developed CAMR within 5 years. Indication biopsies, NER, BS, and TCMR combined. (B) The DSA10 pathway was the most discriminating. Of those above zero score, 51% developed CAMR within 5 years, compared with 14% of those below zero ($P=3.4 \times 10^{-5}$, chi square). *P* values Mann–Whitney. The DSA10 pathway contains ten genes associated with DSA (*CCL4, CD160, CX3CR1, FGFBP2, GBP4, GNLY, PLA1A, ROBO4, SH2D1B, TRDC*).[34]

Table 2. Three-year graft survival after biopsies with CAMR[a] and BS-TCMR[b]

Group	Survive			Fail			P Value	Test
	N	Mean	SD	N	Mean	SD		
CAMR (%)	47			39 (45)				
Age		42.1	17.3		47.1	17	NS	t test
F/M		23/24			11/28		NS	Fisher exact
Years post-tx		7.4	6.6		7.8	5.6	NS	t test
Cr at bx		1.83	0.79		4.59	3.13	8.3×10^{-7}	t test
C4d%		20	29		42	31	2.8×10^{-4}	Mann–Whitney
v score		0.1	0.3		0.4	0.8	0.035	Mann–Whitney
i score		0.9	0.7		1.5	1	0.004	Mann–Whitney
t score		0.8	0.9		1.3	1.2	NS	Mann–Whitney
i-IFTA %		14.9	16.8		26.9	23.7	0.019	t test
% fibrosis		20.5	16.6		29.6	24.4	0.046	t test
mi		3.2	1.5		3.4	1.6	NS	Mann–Whitney
cg		1.7	1.1		1.6	1.2	NS	Mann–Whitney
DSA+/Total tested (%)		41/44 (93)			33/37 (83)		NS	Chi square
BS TCMR (%)	38			12 (24)				
Age		47.9	16.9		37.8	21.9	NS	t test
F/M		15/23			8/4		NS	Fisher exact
rs post-tx		3.4	6.5		4.8	5.4	NS	t test
Cr at bx		2.42	1.45		2.44	1.06	NS	t test
C4d%		0.0	0.0		0.4	0.0	NS	Mann-Whitney
v score		0.3	0.6		0.3	0.5	NS	Mann–Whitney
i score		1.7	0.8		1.6	0.9	NS	Mann-Whitney
t score		1.8	0.8		2.0	1.1	NS	Mann-Whitney
i-IFTA %		8.1	10.7		18.0	18.5	0.081	t test
% fibrosis		10.0	10.5		16.1	19.2	NS	t test
mi		0.2	0.5		0.8	1.2	0.031	Mann-Whitney
cg		0.0	0.1		0.0	0.1	NS	Mann-Whitney
DSA+/Total tested (%)		6/32 (19)			5/12 (42)		0.047	Chi square

[a]Includes mixed rejection (CAMR+TCMR); censored for death with a functioning graft.
[b]BS and TCMR combined; censored for death with a functioning graft.

pathway scores associated with graft loss in the BS-TCMR group but not the CAMR group, whereas higher TCMR pathways associated with graft loss in the CAMR group, but not the TCMR group. This suggests that occult ("subpathological") mixed rejection was present in both groups, not appreciated by pathology criteria. Differential gene expression showed that in both TCMR and CAMR, macrophage transcripts were elevated in the failed-allograft groups, whereas tubule genes were depressed (Supplemental Figures 8 and 9).

To assess the relative contribution of all variables together on 3-year outcome, RF classification was done with combined clinical, laboratory, pathology, pathways, and individual transcript values (Table 3, Supplemental Figures 10 and 11). In the CAMR-mixed group, RF correctly classified 82% of survival cases and 81% of failure cases (81% overall; chi square $P=1.6 \times 10^{-8}$). The top variables were related to injury, repair, macrophages, and TCMR (i). In BS-TCMR, RF accurately classified 85% of the survival cases and 60% of the failure cases (80% overall; chi square $P=1.2 \times 10^{-3}$). Injury, repair, and macrophage transcripts were most prominent, as were variables related to AMR (ptc, endothelium, VWF). When RF classification was used on each variable category separately, those on the

basis of transcripts usually outperformed clinical and pathology variables (Supplemental Table 3).

DISCUSSION

This study provides insights beyond those in microarrays, taking advantage of the ability of nCounter assays to compare pathology results and transcripts on the same tissue sample. Microarray correlations across unselected mixed diagnostic groups reported that ptc, g, cg, and C4d correlated with elevated AMR scores.[10,35,36] In other words, standard histologic diagnosis of AMR correlated with AMR transcripts. We went further to seek evidence for what was driving the elevated AMR transcripts within the CAMR group by comparing progressively increasing pathology scores with quantitative AMR transcript scores. We postulated that the lesions associated with elevation of the transcripts characteristic of AMR would be most related to its pathogenesis. We identified only one Banff pathology lesion that was correlated with AMR pathways in CAMR, namely ptc. Histologic ptc scores from the surface cut of the block used for transcript analysis improved the correlation compared with the scores in the pathology report ($P=9.2 \times 10^{-7}$ versus
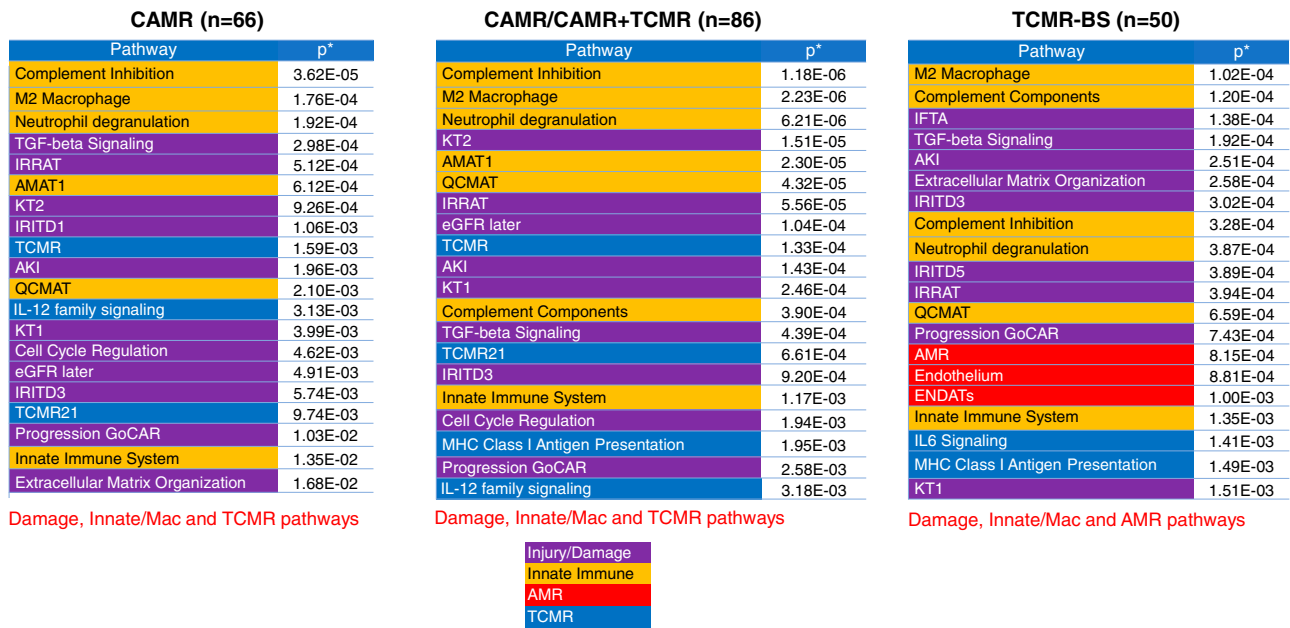
CAMR (n=66)	
Pathway	p*
Complement Inhibition	3.62E-05
M2 Macrophage	1.76E-04
Neutrophil degranulation	1.92E-04
TGF-beta Signaling	2.98E-04
IRRAT	5.12E-04
AMAT1	6.12E-04
KT2	9.26E-04
IRITD1	1.06E-03
TCMR	1.59E-03
AKI	1.96E-03
QCMAT	2.10E-03
IL-12 family signaling	3.13E-03
KT1	3.99E-03
Cell Cycle Regulation	4.62E-03
eGFR later	4.91E-03
IRITD3	5.74E-03
TCMR21	9.74E-03
Progression GoCAR	1.03E-02
Innate Immune System	1.35E-02
Extracellular Matrix Organization	1.68E-02

Damage, Innate/Mac and TCMR pathways

CAMR/CAMR+TCMR (n=86)	
Pathway	p*
Complement Inhibition	1.18E-06
M2 Macrophage	2.23E-06
Neutrophil degranulation	6.21E-06
KT2	1.51E-05
AMAT1	2.30E-05
QCMAT	4.32E-05
IRRAT	5.56E-05
eGFR later	1.04E-04
TCMR	1.33E-04
AKI	1.43E-04
KT1	2.46E-04
Complement Components	3.90E-04
TGF-beta Signaling	4.39E-04
TCMR21	6.61E-04
IRITD3	9.20E-04
Innate Immune System	1.17E-03
Cell Cycle Regulation	1.94E-03
MHC Class I Antigen Presentation	1.95E-03
Progression GoCAR	2.58E-03
IL-12 family signaling	3.18E-03

Damage, Innate/Mac and TCMR pathways

TCMR-BS (n=50)	
Pathway	p*
M2 Macrophage	1.02E-04
Complement Components	1.20E-04
IFTA	1.38E-04
TGF-beta Signaling	1.92E-04
AKI	2.51E-04
Extracellular Matrix Organization	2.58E-04
IRITD3	3.02E-04
Complement Inhibition	3.28E-04
Neutrophil degranulation	3.87E-04
IRITD5	3.89E-04
IRRAT	3.94E-04
QCMAT	6.59E-04
Progression GoCAR	7.43E-04
AMR	8.15E-04
Endothelium	8.81E-04
ENDATs	1.00E-03
Innate Immune System	1.35E-03
IL6 Signaling	1.41E-03
MHC Class I Antigen Presentation	1.49E-03
KT1	1.51E-03

Damage, Innate/Mac and AMR pathways

Injury/Damage
Innate Immune
AMR
TCMR

Figure 8. Top 20 pathways that correlate with 3-year graft failure. The 20 pathways (gene sets) that were most associated with 3-year graft failure of CAMR, mixed (CAMR+TCMR), and BS-TCMR (borderline for rejection and TCMR) are listed. Damage, innate, and M2 macrophage pathways are correlated with graft failure in all groups. TCMR but not AMR pathways correlate with failure in the CAMR and mixed (CAMR+TCMR) group, whereas AMR pathways and not TCMR pathways correlate with graft failure in the BS-TCMR group. This argues that subliminal TCMR or AMR revealed by transcripts, but not appreciated by histology, influences the outcome.

3.0×10^{-4}). Glomerular inflammation (g) correlated only weakly or not at all with AMR scores, even when scored on the surface cuts from nCounter blocks ($P=0.08$ versus 0.07). This may be due to the relatively crude Banff g scoring method, the lower number of glomerular capillaries compared with ptc, or a qualitatively different glomerular response. Thus, the mi score (g+ptc) was somewhat less correlated with AMR transcripts ($P=7.2 \times 10^{-5}$) than ptc scores alone. No correlation was evident with cg, v, C4d extent, or other Banff scores within the CAMR diagnostic group.

Microarray studies discovered that transcripts in CAMR are primarily related to endothelium and NK cells.[27] We have confirmed those results in the CAMR group. The strongest correlation with ptc scores in CAMR were with NK and Endothelial transcripts ($P=4.2 \times 10^{-9}$ and 3.2×10^{-9}, respectively). These results are consistent with experimental evidence in mice that NK cells mediate chronic AMR via ADCC independent of complement activation.[37,38] Increased NK and endothelial transcripts were present even in CAMR biopsies with ptc0, indicating some

Table 3. Outcome reclassification with RF

	Outcome Observed[a]			
RF Classification	Survive	Fail	Total	% Correct with RF Classification
BS TCMR				
Survive	40	9	49	82
Fail	7	30	37	81
Total	47	39	86	81
% correct without RF	55	45		
			Chi square[a]	1.6×10^{-8}
BS TCMR				
Survive	34	6	40	85
Fail	4	6	10	60
Total	38	12	50	80
% correct without RF	76	24		
			Chi square[a]	1.2×10^{-2}

[a]Includes mixed rejection (CAMR+TCMR); censored for death with a functioning graft.

transcript effect occurs below the Banff threshold of ptc1. This argues for seeking improved sensitivity and precision in the assessment of ptc.[39,40]

No transcript response could be connected with C4d deposition in CAMR: even C4d0 biopsies had a maximal AMR transcript response. Furthermore, no AMR transcript response was evident in C4d+ ABOi grafts. The results argue that complement activation does not contribute to the pathogenesis of CAMR. Our results do not exclude the possibility that other genes that are not in the B-HOT panel may be affected by complement deposition. C4d did correlate with graft loss and the presence of TCMR in CAMR. Some, but not all studies have concluded that more severe disease is associated with C4d deposition.[6,41] This contrasts with acute AMR in presensitized patients in which AMR transcripts correlate with C4d and not ptc,[42] evidence of a complement-driven process in this setting. A possible explanation is that the endothelium becomes more resistant to complement effects in chronic exposure to DSA.[43]

DSA was correlated with AMR transcripts in CAMR. The patients with DSA⁻ CAMR showed a lower level of AMR transcripts than DSA⁺ CAMR, but were still significantly elevated when compared with patients with non-CAMR. This suggests the pathophysiology of DSA⁻ CAMR differs quantitatively, but not qualitatively, from DSA⁺ CAMR. This is compatible with the report that DSA⁻ CAMR has a better prognosis than DSA⁺ CAMR.[44,45]

Peritubular capillaritis and DSA were the principal correlates of AMR transcript elevation, but this does not prove causation. Elevation of the AMR pathway scores in the CAMR ptc0 group suggests other factors, for example, DSA may be the primary stimulus or that pathogenetically significant capillaritis may be present below current criteria. DSA alone causes transcript elevation and promotion of monocyte recruitment in cultured endothelium, and would therefore be a plausible primary event.[18,19] We interpret the progressive rise in endothelial transcripts with increase capillaritis as evidence that capillaritis potentiates the endothelial response, presumably by Fc receptor bearing mononuclear cells (NK and macrophages). More definitive evidence of these hypotheses may be revealed by spatial analysis of transcripts and selective inhibitors of ADCC.

EHD3 and *SOST* are expressed specifically in glomerular endothelium[30,31] and show progressive loss with increasing cg scores. *EHD3* encodes a protein thought to be involved in endocytic trafficking.[46] Inactivation of *Ehd3* along with the related *Ehd4* in mice results in glomerular endothelial changes indistinguishable from transplant glomerulopathy, including loss of fenestrations, expansion of cytoplasm, and duplication of the GBM.[47] This raises the possibility that *EHD3* is involved in the pathogenic pathway of transplant glomerulopathy. *SOST* (sclerostin) codes for a WNT inhibitor expressed in osteocytes.[48] Microarray studies noted a decrease in *SOST* transcripts in AMR[27] and subsequent single-cell RNA analysis revealed *SOST* is expressed in selectively in glomerular endothelial cells.[30] The role of SOST in glomerular endothelium physiology is unknown.

The results from patients that later developed CAMR provide proof that transcripts can detect relevant pathophysiologic mechanisms not appreciable by standard pathology criteria. There are limits to this predictive power, however. CAMR developing beyond 5 years showed no signal, and presumably had not begun at the time of the biopsy. About half of the patients with elevated AMR transcripts did not have a later biopsy documenting CAMR in the follow-up period. We could not distinguish whether these patients later had subclinical CAMR that was not biopsied, or whether the cause of the initial transcript elevation resolved. DSA levels at the time of the biopsy were less predictive of CAMR than AMR transcripts. These results are considered preliminary until validated in an independent sample.

Graft failure within 3 years of biopsies showing CAMR or BS-TCMR was associated with multiple damage pathways derived from microarray studies, such as KT1, KT2,[49] IRRAT,[25] IRIT1,3,5,[50] eGFR later,[51] and Progression GoCAR.[32,33] Einecke showed similar findings and emphasized that damage was more relevant to outcome than AMR pathway activity in CAMR.[25] Our data agree and show in addition that TCMR pathways in BS-TCMR had no correlation with outcome. Our results reveal the novel finding that elevation of TCMR pathways in CAMR or AMR pathways in BS-TCMR correlated with adverse outcomes, indicating transcripts can detect clinically significant subliminal mixed rejection not appreciated by Banff criteria. Injury may cause the TCMR pathway elevation rather than TCMR itself. As expected, overt mixed rejection by Banff criteria also had a worse outcome than CAMR alone, and individual features that were suggestive of, but not sufficient for, a diagnosis of mixed rejection (mi and DSA in BS-TCMR).

This study did not survey all of the pathologies of renal allografts, because our goal was to reveal mechanisms and outcome. We did not subdivide patients into further categories on the basis of MHC match, therapy, or other variables. A more sophisticated analysis and validation of these results is planned for the larger dataset that is accumulating in the International Consortium for Diagnosis and Outcome in Transplantation.[9]

The RF classification correctly identified the outcome of 3-year graft failure or survival in 81% and 80% of the cases of CAMR-mixed and BS-TCMR, respectively. Transcripts, pathology, and clinical variables all contributed, although the transcript-based variables usually outperformed the clinical and pathology variables. Both diagnostic groups were influenced by transcripts related to injury, repair, and macrophages. Some predictive variables were different. For CAMR-mixed cases, TCMR-related variables (i), serum Cr, %C4d, complement inhibition, and glomerular endothelium pathways were important. For BS-TCMR, AMR-related

variables (ptc, pan-endothelium, VWF) were important. Variables not included in our RF may contribute to misclassification. A combined clinical, pathologic, and molecular RF approach to risk assessment has some promise, but will need confirmation and refinement.

DISCLOSURES

FUNDING

ACKNOWLEDGEMENTS

AUTHOR CONTRIBUTIONS

R.B. Colvin conceptualized the study; A. Benedict Cosimi, R.B. Colvin, N. Elias, H. Gilligan, K. Hotta, N. Iwahara, T. Kawai, G.K. Mahowald, T. Otsuka, L. Riella, I. Rosales, K. Safa, N. Smith, Y. Takada, N. Tolkoff-Rubin, K. Tomaszewski, T. Tsuji, and W.W. Williams were responsible for the data curation; R.B. Colvin and N. Smith were responsible for the formal analysis; R.B. Colvin was responsible for the funding acquisition; R.B. Colvin, K. Hotta, N. Iwahara, G.K. Mahowald, T. Otsuka, I. Rosales, N. Smith, Y. Takada, K. Tomaszewski, and T. Tsuji were responsible for the investigation; E. Acheampong, M. Araujo Medina, A. Bruce, K. Hotta, N. Iwahara, G.K. Mahowald, T. Otsuka, A. Rios, I. Rosales, Y. Takada, K. Tomaszewski, and T. Tsuji were responsible for the methodology; K. Hotta, N. Iwahara, T. Otsuka, I. Rosales, Y. Takada, K. Tomaszewski, and T. Tsuji were responsible for the project administration; R.B. Colvin provided supervision; R.B. Colvin was responsible for the visualization; R.B. Colvin and I. Rosales wrote original draft; A. Benedict Cosimi, R.B. Colvin, N. Elias, H. Gilligan, K. Hotta, N. Iwahara, T. Kawai, G.K. Mahowald, T. Otsuka, L. Riella, I. Rosales, K. Safa, N. Smith, N. Tolkoff-Rubin, K. Tomaszewski, T. Tsuji, and W.W. Williams reviewed and edited the manuscript.

DATA SHARING STATEMENT

All data used in this study are available in this article.

SUPPLEMENTAL MATERIAL

This article contains the following supplemental material online at http://jasn.asnjournals.org/lookup/suppl/doi:10.1681/ASN.2022040444/-/DCSupplemental

Supplemental Table 1. Aggregate Banff scores and other pathology features by diagnostic category.

Supplemental Table 2. HOT panel pathway gene sets.

Supplemental Table 3. RF % correct classification of 3-year graft survival by variable type.

Supplemental Table 4. Univariate analysis of all variables. No CAMR versus PreCAMR within 5 years.

Supplemental Figure 1. HK normalization corrects block age effect on RNA recovery.

Supplemental Figure 2. AMR pathways are not affected by t in CAMR whereas TCMR pathways correlate with t.

Supplemental Figure 3. AMR pathway scores not correlated with glomerular i (Banff g scores).

Supplemental Figure 4. AMR pathway scores are not correlated with endarteritis (v score) in CAMR.

Supplemental Figure 5. Differential gene expression in DSA^+ and DSA^- CAMR.

Supplemental Figure 6. Prediction of CAMR declines progressively with later onset.

Supplemental Figure 7. M2 macrophage subset is associated with graft failure.

Supplemental Figure 8. Differential gene expression in CAMR is associated with graft failure 3 years after biopsy (indication biopsies).

Supplemental Figure 9. Differential gene expression in TCMR is associated with graft failure 3 years after biopsy (indication biopsies).

Supplemental Figure 10. RF outcome classification in CAMR/Mixed.

Supplemental Figure 11. RF outcome classification in BS-TCMR.

Supplemental Figure 12. RF outcome classification in CAMR/Mixed using each category of variables.

Supplemental Figure 13. RF outcome classification in BS-TCMR using each category of variables.

REFERENCES

1. Mauiyyedi S, Pelle PD, Saidman S, Collins AB, Pascual M, Tolkoff-Rubin NE, et al.: Chronic humoral rejection: Identification of antibody-mediated chronic renal allograft rejection by C4d deposits in peritubular capillaries. *J Am Soc Nephrol* 12: 574–582, 2001

2. Regele H, Böhmig GA, Habicht A, Gollowitzer D, Schillinger M, Rockenschaub S, et al.: Capillary deposition of complement split product C4d in renal allografts is associated with basement

membrane injury in peritubular and glomerular capillaries: A contribution of humoral immunity to chronic allograft rejection. *J Am Soc Nephrol* 13: 2371–2380, 2002

3. Solez K, Colvin RB, Racusen LC, Sis B, Halloran PF, Birk PE, et al.: Banff '05 Meeting Report: Differential diagnosis of chronic allograft injury and elimination of chronic allograft nephropathy ('CAN'). *Am J Transplant* 7: 518–526, 2007

4. Einecke G, Sis B, Reeve J, Mengel M, Campbell PM, Hidalgo LG, et al.: Antibody-mediated microcirculation injury is the major cause of late kidney transplant failure. *Am J Transplant* 9: 2520–2531, 2009

5. Gaston RS, Cecka JM, Kasiske BL, Fieberg AM, Leduc R, Cosio FC, et al.: Evidence for antibody-mediated injury as a major determinant of late kidney allograft failure. *Transplantation* 90: 68–74, 2010

6. Wiebe C, Gibson IW, Blydt-Hansen TD, Karpinski M, Ho J, Storsley LJ, et al.: Evolution and clinical pathologic correlations of de novo donor-specific HLA antibody post kidney transplant. *Am J Transplant* 12: 1157–1167, 2012

7. Farkash EA, Colvin RB: Diagnostic challenges in chronic antibody-mediated rejection. *Nat Rev Nephrol* 8: 255–257, 2012

8. Matignon M, Muthukumar T, Seshan SV, Suthanthiran M, Hartono C: Concurrent acute cellular rejection is an independent risk factor for renal allograft failure in patients with C4d-positive antibody-mediated rejection. *Transplantation* 94: 603–611, 2012

9. Mengel M, Loupy A, Haas M, Roufosse C, Naesens M, Akalin E, et al.: Banff 2019 Meeting Report: Molecular diagnostics in solid organ transplantation-Consensus for the Banff Human Organ Transplant (B-HOT) gene panel and open source multicenter validation. *Am J Transplant* 20: 2305–2317, 2020

10. Sis B, Jhangri GS, Bunnag S, Allanach K, Kaplan B, Halloran PF: Endothelial gene expression in kidney transplants with alloantibody indicates antibody-mediated damage despite lack of C4d staining. *Am J Transplant* 9: 2312–2323, 2009

11. Bröcker V, Pfaffenbach A, Habicht A, Chatzikyrkou C, Kreipe HH, Haller H, et al.: Beyond C4d: The ultrastructural appearances of endothelium in ABO-incompatible renal allografts. *Nephrol Dial Transplant* 28: 3101–3109, 2013

12. Stegall MD, Diwan T, Raghavaiah S, Cornell LD, Burns J, Dean PG, et al.: Terminal complement inhibition decreases antibody-mediated rejection in sensitized renal transplant recipients. *Am J Transplant* 11: 2405–2413, 2011

13. Dean PG, Park WD, Cornell LD, Schinstock CA, Stegall MD: Early subclinical inflammation correlates with outcomes in positive crossmatch kidney allografts. *Clin Transplant* 30: 925–933, 2016

14. Marks WH, Mamode N, Montgomery RA, Stegall MD, Ratner LE, Cornell LD, et al; C10-001 Study Group: Safety and efficacy of eculizumab in the prevention of antibody-mediated rejection in living-donor kidney transplant recipients requiring desensitization therapy: A randomized trial. *Am J Transplant* 19: 2876–2888, 2019

15. Loupy A, Hill GS, Suberbielle C, Charron D, Anglicheau D, Zuber J, et al.: Significance of C4d Banff scores in early protocol biopsies of kidney transplant recipients with preformed donor-specific antibodies (DSA). *Am J Transplant* 11: 56–65, 2011

16. Hidalgo LG, Sellares J, Sis B, Mengel M, Chang J, Halloran PF: Interpreting NK cell transcripts versus T cell transcripts in renal transplant biopsies. *Am J Transplant* 12: 1180–1191, 2012

17. Hidalgo LG, Sis B, Sellares J, Campbell PM, Mengel M, Einecke G, et al.: NK cell transcripts and NK cells in kidney biopsies from patients with donor-specific antibodies: Evidence for NK cell involvement in antibody-mediated rejection. *Am J Transplant* 10: 1812–1822, 2010

18. Valenzuela NM, Trinh KR, Mulder A, Morrison SL, Reed EF: Monocyte recruitment by HLA IgG-activated endothelium: The relationship between IgG subclass and FcγRIIa polymorphisms. *Am J Transplant* 15: 1502–1518, 2015

19. Zhang X, Reed EF: Effect of antibodies on endothelium. *Am J Transplant* 9: 2459–2465, 2009

20. Loupy A, Haas M, Roufosse C, Naesens M, Adam B, Afrouzian M, et al.: The Banff 2019 Kidney Meeting Report (I): Updates on and clarification of criteria for T cell- and antibody-mediated rejection. *Am J Transplant* 20: 2318–2331, 2020

21. Adam BA, Smith RN, Rosales IA, Matsunami M, Afzali B, Oura T, et al.: Chronic antibody-mediated rejection in nonhuman primate renal allografts: Validation of human histological and molecular phenotypes. *Am J Transplant* 17: 2841–2850, 2017

22. Halloran PF, Matas A, Kasiske BL, Madill-Thomsen KS, Mackova M, Famulski KS: Molecular phenotype of kidney transplant indication biopsies with inflammation in scarred areas. *Am J Transplant* 19: 1356–1370, 2019

23. Halloran PF, Venner JM, Madill-Thomsen KS, Einecke G, Parkes MD, Hidalgo LG, et al.: Review: The transcripts associated with organ allograft rejection. *Am J Transplant* 18: 785–795, 2018

24. Halloran PF, Venner JM, Famulski KS: Comprehensive analysis of transcript changes associated with allograft rejection: Combining universal and selective features. *Am J Transplant* 17: 1754–1769, 2017

25. Einecke G, Reeve J, Gupta G, Bohmig GA, Eskandary F, Bromberg JS, et al.: Factors associated with kidney graft survival in pure antibody-mediated rejection at the time of indication biopsy: Importance of parenchymal injury but not disease activity. *Am J Transplant* 21: 1391–1404, 2020

26. Tomfohr J, Lu J, Kepler TB: Pathway level analysis of gene expression using singular value decomposition. *BMC Bioinformatics* 6: 225, 2005

27. Venner JM, Hidalgo LG, Famulski KS, Chang J, Halloran PF: The molecular landscape of antibody-mediated kidney transplant rejection: Evidence for NK involvement through CD16a Fc receptors. *Am J Transplant* 15: 1336–1348, 2015

28. Smith RN, Matsunami M, Adam BA, Rosales IA, Oura T, Cosimi AB, et al.: RNA expression profiling of nonhuman primate renal allograft rejection identifies tolerance. *Am J Transplant* 18: 1328–1339, 2018

29. Mengel M, Reeve J, Bunnag S, Einecke G, Jhangri GS, Sis B, et al.: Scoring total inflammation is superior to the current Banff inflammation score in predicting outcome and the degree of molecular disturbance in renal allografts. *Am J Transplant* 9: 1859–1867, 2009

30. Menon R, Otto EA, Hoover P, Eddy S, Mariani L, Godfrey B, et al; Nephrotic Syndrome Study Network (NEPTUNE): Single cell transcriptomics identifies focal segmental glomerulosclerosis remission endothelial biomarker. *JCI Insight* 5: 133267, 2020

31. Patrakka J, Xiao Z, Nukui M, Takemoto M, He L, Oddsson A, et al.: Expression and subcellular distribution of novel glomerulus-associated proteins dendrin, ehd3, sh2d4a, plekhh2, and 2310066E14Rik. *J Am Soc Nephrol* 18: 689–697, 2007

32. O'Connell PJ, Zhang W, Menon MC, Yi Z, Schröppel B, Gallon L, et al.: Biopsy transcriptome expression profiling to identify kidney transplants at risk of chronic injury: A multicentre, prospective study. *Lancet* 388: 983–993, 2016

33. Menon MC, Chuang PY, Li Z, Wei C, Zhang W, Luan Y, et al.: Intronic locus determines SHROOM3 expression and potentiates renal allograft fibrosis. *J Clin Invest* 125: 208–221, 2015

34. Madill-Thomsen KS, Böhmig GA, Bromberg J, Einecke G, Eskandary F, Gupta G, et al; INTERCOMEX Investigators: Donor-specific antibody is associated with increased expression of rejection transcripts in renal transplant biopsies classified as no rejection. *J Am Soc Nephrol* 32: 2743–2758, 2021

35. Halloran PF, Pereira AB, Chang J, Matas A, Picton M, De Freitas D, et al.: Microarray diagnosis of antibody-mediated rejection in kidney transplant biopsies: An international prospective study (INTERCOM). *Am J Transplant* 13: 2865–2874, 2013

36. Sellarés J, Reeve J, Loupy A, Mengel M, Sis B, Skene A, et al.: Molecular diagnosis of antibody-mediated rejection in human kidney transplants. *Am J Transplant* 13: 971–983, 2013

37. Hirohashi T, Chase CM, Della Pelle P, Sebastian D, Alessandrini A, Madsen JC, et al.: A novel pathway of chronic allograft rejection mediated by NK cells and alloantibody. *Am J Transplant* 12: 313–321, 2012

38. Lin CM, Plenter RJ, Coulombe M, Gill RG: Interferon gamma and contact-dependent cytotoxicity are each rate limiting for natural killer cell-mediated antibody-dependent chronic rejection. *Am J Transplant* 16: 3121–3130, 2016

39. Delsante M, Maggiore U, Levi J, Kleiner DE, Jackson AM, Arend LJ, et al.: Microvascular inflammation in renal allograft biopsies assessed by endothelial and leukocyte co-immunostain: A retrospective study on reproducibility and clinical/prognostic correlates. *Transpl Int* 32: 300–312, 2019

40. Kozakowski N, Herkner H, Böhmig GA, Regele H, Kornauth C, Bond G, et al.: The diffuse extent of peritubular capillaritis in renal allograft rejection is an independent risk factor for graft loss. *Kidney Int* 88: 332–340, 2015

41. Cohen D, Colvin RB, Daha MR, Drachenberg CB, Haas M, Nickeleit V, et al.: Pros and cons for C4d as a biomarker. *Kidney Int* 81: 628–639, 2012

42. Loupy A, Lefaucheur C, Vernerey D, Chang J, Hidalgo LG, Beuscart T, et al.: Molecular microscope strategy to improve risk stratification in early antibody-mediated kidney allograft rejection. *J Am Soc Nephrol* 25: 2267–2277, 2014

43. Chen Song S, Zhong S, Xiang Y, Li JH, Guo H, Wang WY, et al.: Complement inhibition enables renal allograft accommodation and long-term engraftment in presensitized nonhuman primates. *Am J Transplant* 11: 2057–2066, 2011

44. Senev A, Van Loon E, Lerut E, Callemeyn J, Coemans M, Van Sandt V, et al.: Risk factors, histopathological features, and graft outcome of transplant glomerulopathy in the absence of donor-specific HLA antibodies. *Kidney Int* 100: 401–414, 2021

45. Sablik KA, Clahsen-van Groningen MC, Looman CWN, Damman J, Roelen DL, van Agteren M, et al.: Chronic-active antibody-mediated rejection with or without donor-specific antibodies has similar histomorphology and clinical outcome - a retrospective study. *Transpl Int* 31: 900–908, 2018

46. Zhang L, Ding L, Li Y, Zhang F, Xu Y, Pan H, et al.: EHD3 positively regulated by NR5A1 participates in testosterone synthesis via endocytosis. *Life Sci* 278: 119570, 2021

47. George M, Rainey MA, Naramura M, Foster KW, Holzapfel MS, Willoughby LL, et al.: Renal thrombotic microangiopathy in mice with combined deletion of endocytic recycling regulators EHD3 and EHD4. *PLoS One* 6: e17838, 2011

48. Nguyen-Yamamoto L, Tanaka KI, St-Arnaud R, Goltzman D: Vitamin D-regulated osteocytic sclerostin and BMP2 modulate uremic extraskeletal calcification. *JCI Insight* 4: 126467, 2019

49. Einecke G, Kayser D, Vanslambrouck JM, Sis B, Reeve J, Mengel M, et al.: Loss of solute carriers in T cell-mediated rejection in mouse and human kidneys: An active epithelial injury-repair response. *Am J Transplant* 10: 2241–2251, 2010

50. Famulski KS, Broderick G, Einecke G, Hay K, Cruz J, Sis B, et al.: Transcriptome analysis reveals heterogeneity in the injury response of kidney transplants. *Am J Transplant* 7: 2483–2495, 2007

51. Vitalone MJ, Ganguly B, Hsieh S, Latek R, Kulbokas EJ, Townsend R, et al.: Transcriptional profiling of belatacept and calcineurin inhibitor therapy in renal allograft recipients. *Am J Transplant* 14: 1912–1921, 2014

AFFILIATIONS

[1]Department of Pathology, Massachusetts General Hospital and Harvard Medical School, Boston, Massachusetts

[2]Center for Transplantation Sciences, Department of Surgery, Massachusetts General Hospital and Harvard Medical School, Boston, Massachusetts

[3]Department of Urology, Hokkaido University Hospital, Hokkaido, Japan

[4]Department of Surgical Pathology, Hokkaido University Hospital, Hokkaido, Japan

[5]Department of Pathology, Sapporo City General Hospital, Hokkaido, Japan

[6]Department of Kidney Transplant Surgery, Sapporo City General Hospital, Hokkaido, Japan

[7]Division of Nephrology, Massachusetts General Hospital and Harvard Medical School, Boston, Massachusetts

Supplemental Figure Legends

Supplemental Figure 1. HK normalization corrects block age effect on RNA recovery. Plotted are the log2 geometric means of 758 gene probes from 301 needle core kidney biopsies by age of block. The yield of RNA without housekeeping normalization shows a steady decline. Normalization using 12 housekeeping (HK) genes per the standard normalization procedure corrects this effect. (Pearson correlation coefficient, r).

Supplemental Figure 2. AMR pathways are not affected by tubulitis in CAMR while TCMR pathways correlate with tubulitis. A) AMR pathway scores do not correlate with tubulitis (Banff t) in CAMR. B) TCMR pathways correlate with tubulitis. TCMR pathway scores show a strong correlation with the extent of tubulitis whether in CAMR or non-CAMR. (p values by logistic regression).

Supplemental Figure 3. AMR pathway scores not correlated with glomerular inflammation (Banff g scores). A) AMR pathway scores are not correlated with glomerulitis (Banff g) in CAMR. B) Pan-Endothelium pathway scores are not correlated with transplant glomerulopathy scores (Banff cg). (p values by logistic regression, red; Mann-Whitney, blue).

Supplemental Figure 4: AMR pathway scores are not correlated with endarteritis (v score) and glomerular basement membrane duplication (cg score) in CAMR. A) AMR pathway scores are not correlated with endarteritis (v score) in TCMR or CAMR. B) TCMR pathway scores correlate with the presence of endarteritis in TCMR and Mixed rejection. (p values by logistic regression, red; Mann-Whitney, blue).

Supplemental Figure 5: Differential Gene Expression in DSA⁺ Positive and DSA⁻ CAMR. Four endothelial genes are differentially expressed. Six genes were differentially expressed in DSA⁺ CAMR related to NK cells, endothelium and lymphocyte chemotaxis/angiogenesis. One gene was elevated in DSA neg CAMR, the hepatocyte growth factor receptor (MET) typically expressed in epithelial cells, including proximal tubular epithelium.

Supplemental Figure 6. M2 Macrophage Subset is associated with graft failure. Macrophage gene sets associated with M2 but not M1 macrophages are elevated in biopsies with TCMR or CAMR that fail within 3 years. Genes in the panels are indicated. M2 but not M1 macrophage scores were correlated with outcome in both TCMR and CAMR (with or without TCMR). (p values, two tailed t test).

Supplemental Figure 7. Differential gene expression in CAMR is associated with graft failure 3 years after biopsy (indication biopsies). Several macrophage associated genes are elevated in grafts that failed (green highlight).

Supplemental Figure 8. Differential gene expression in TCMR is associated with graft failure 3 years after biopsy (indication biopsies). Several macrophage associated genes are elevated in grafts that failed (green highlight).

Supplemental Figure 9. Prediction of CAMR declines progressively with later onset. A and B) AMR pathway scores in samples with a diagnosis of NER, BS or TCMR decrease with later onset of CAMR. (p values by logistic regression, red; Mann-Whitney, blue).

Supplemental Figure 10. Random Forest Outcome Classification in CAMR/Mixed.

Representative RF classification of outcome in CAMR/Mixed cases using the top 24 variables selected from all variables combined (clinical, pathology, pathway/cell types and individual genes (n=953) (see Supplemental Figure 12 A-D). All types of variables contributed. The variables are ranked by relative importance to the correct RF classification and color-coded by type. All variables are higher in the Fail group except KT2, Glomerular Endothelium, *FCER1A, PDGFRB, IFIT1, CD207, and SLC4A1.* Seventy random samples were used to generate 2000 different trees and then classify the samples which were not used to generate each tree (the Out Of Bag samples, OOB). Details are given in the Methods section.

Supplemental Figure 11. Random Forest Outcome Classification in BS-TCMR.

Representative RF classification of outcome in BS-TCMR cases using the top 33 variables selected from all variables combined (clinical, pathology, pathway/cell types and individual genes (n=953) (see Supplemental Figure 13 A-D). All types of variables contributed except the clinical/laboratory variables. The variables are ranked by relative importance to the correct RF classification and color-coded by type. All variables are higher in Fail group, except Banff i.

Thirty-five random samples were used to generate 2000 different trees and then classify the samples which were not used to generate each tree (the Out Of Bag samples, OOB). Details are given in the Methods section.

Supplemental Figure 12. Random Forest Outcome Classification in CAMR/Mixed Using Each Category of Variables. Top variables are listed from A) Clinical and

Laboratory Variables B) Pathology C) Pathway/Cell type Scores D) Individual Transcripts.

Supplemental Figure 13. Random Forest Outcome Classification in BS-TCMR Using Each Category of Variables. Top variables are listed from A) Clinical and Laboratory Variables B) Pathology C) Pathway/Cell Type Scores and D) Individual Transcripts.

Supplemental Table 1. Aggregate Banff scores and other pathology features by diagnostic category.

Supplemental Table 2. HOT Panel Pathway Gene Sets. Includes NanoString Advanced Analysis Pathways and cell types, published transplant gene sets (Microarray, nCounter) and custom gene sets and cell types (Colvin et al).

Supplemental Table 3. Random Forest % Correct Classification of 3-Year Graft Survival by Variable Type.
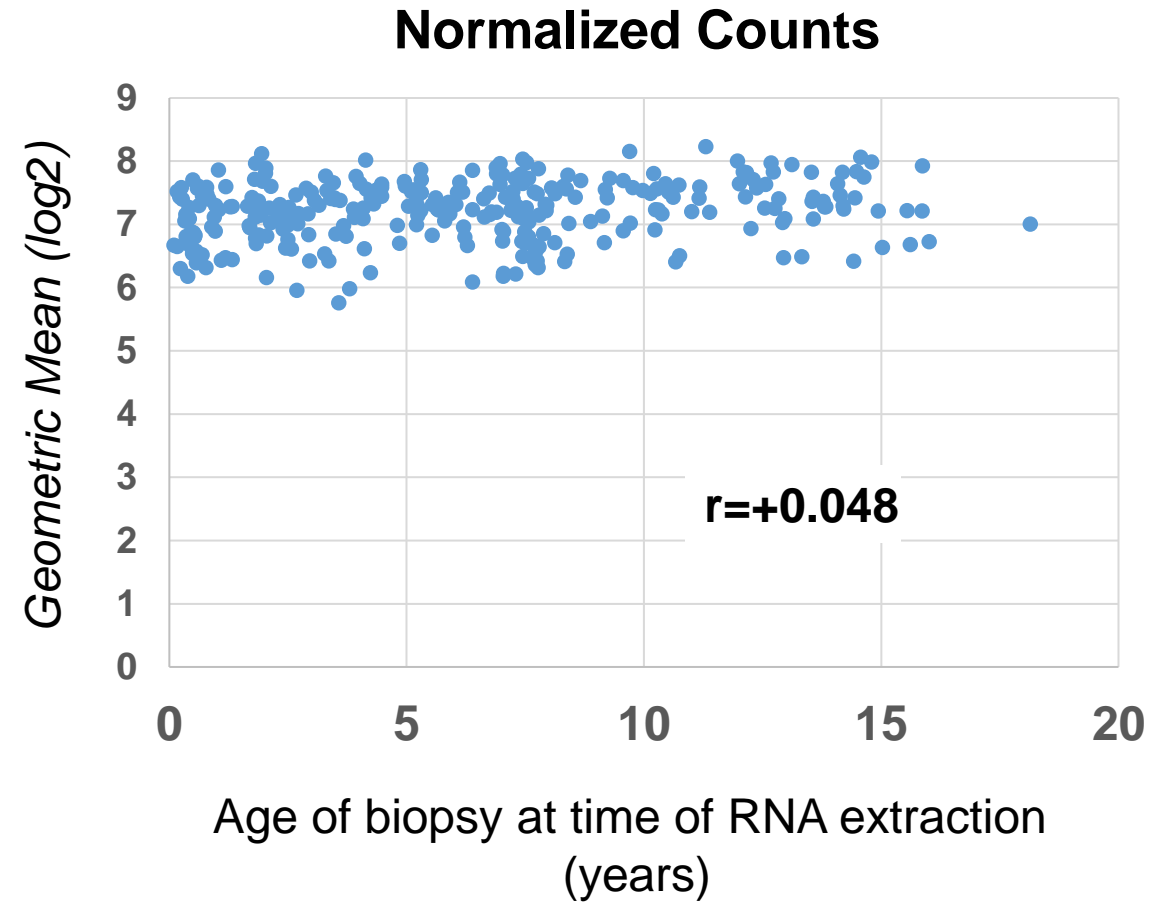
Supplemental Table 4. Univariate analysis of all variables: No CAMR vs PreCAMR within 5 years.
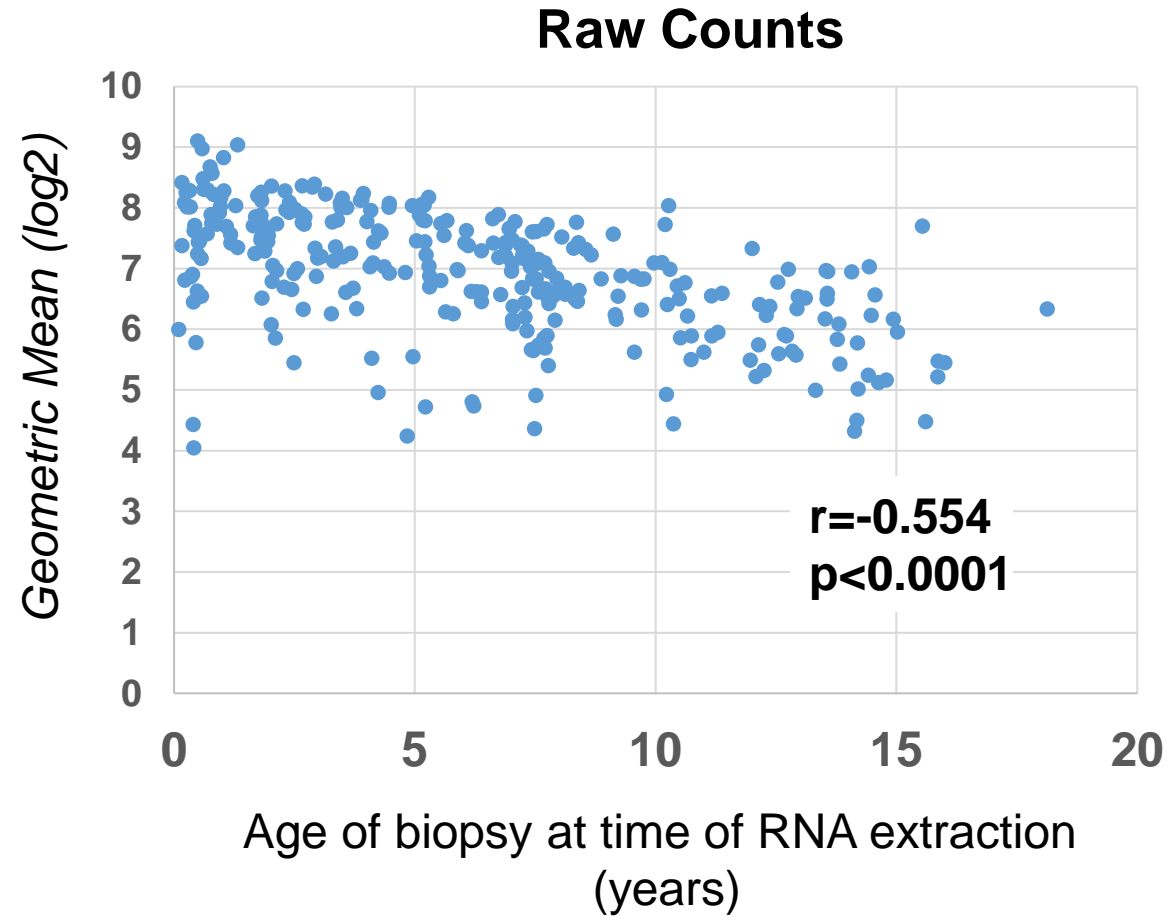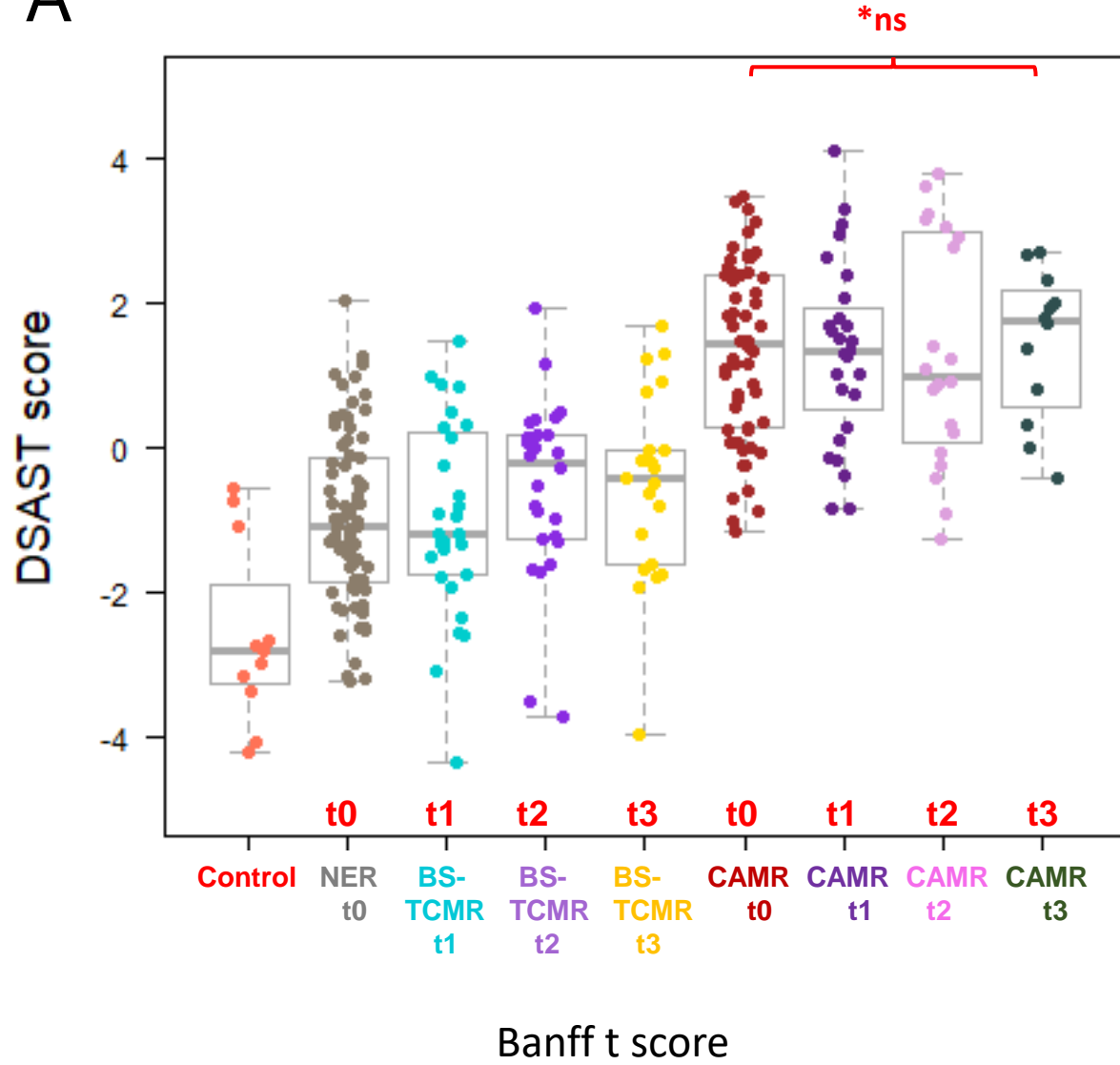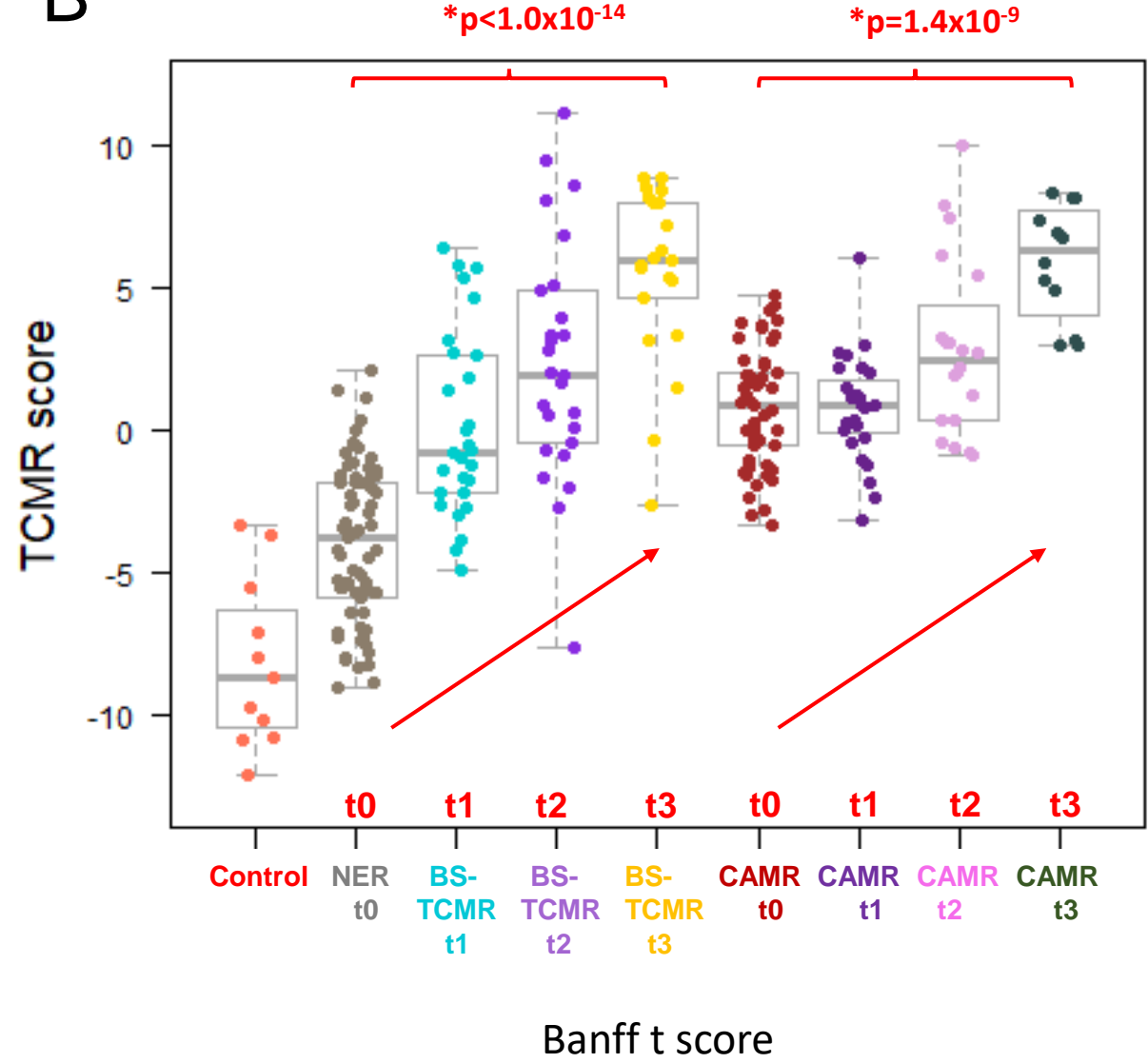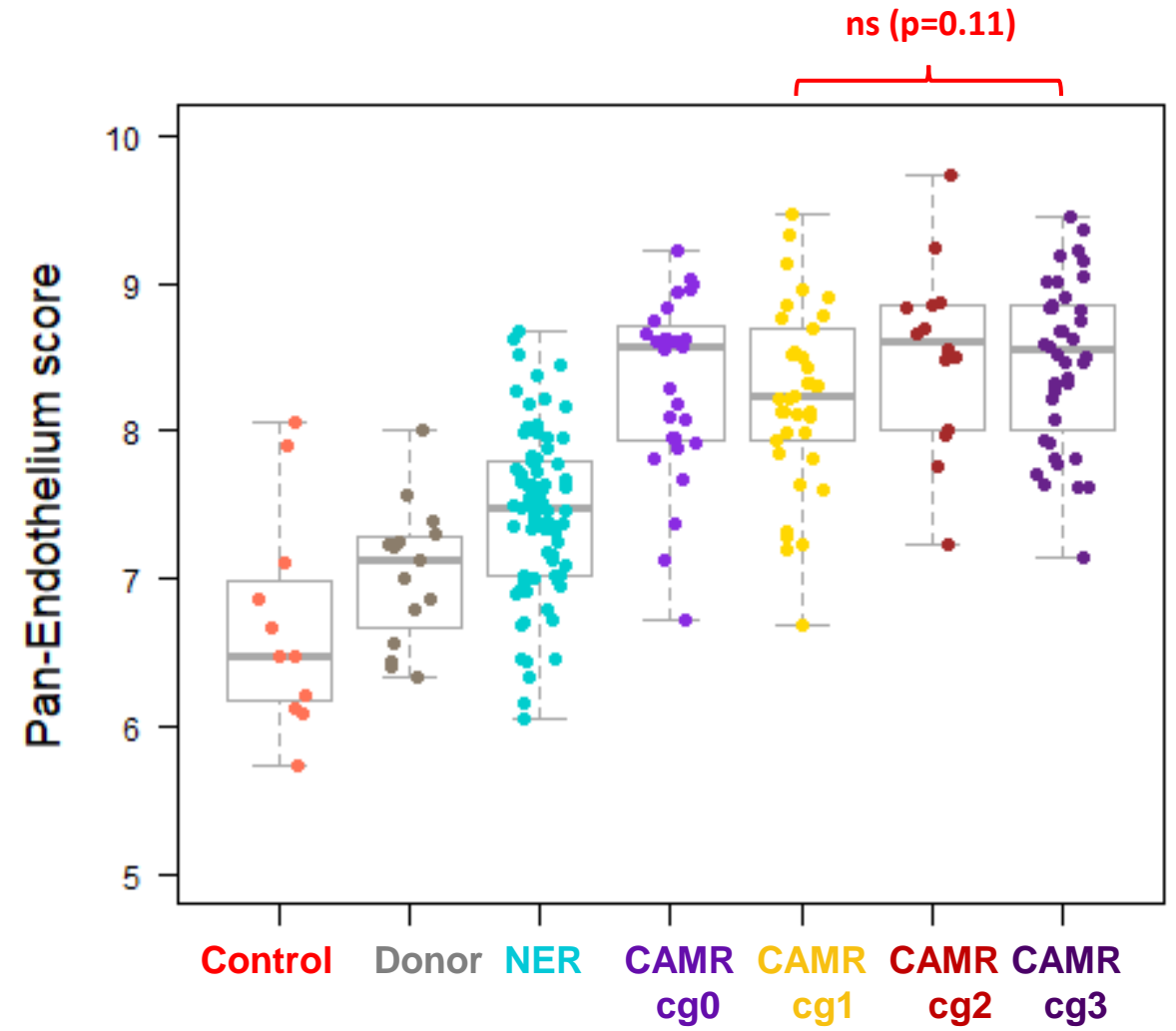
Supplemental Figure 1

Supplemental Figure 2

Supplemental Figure 3
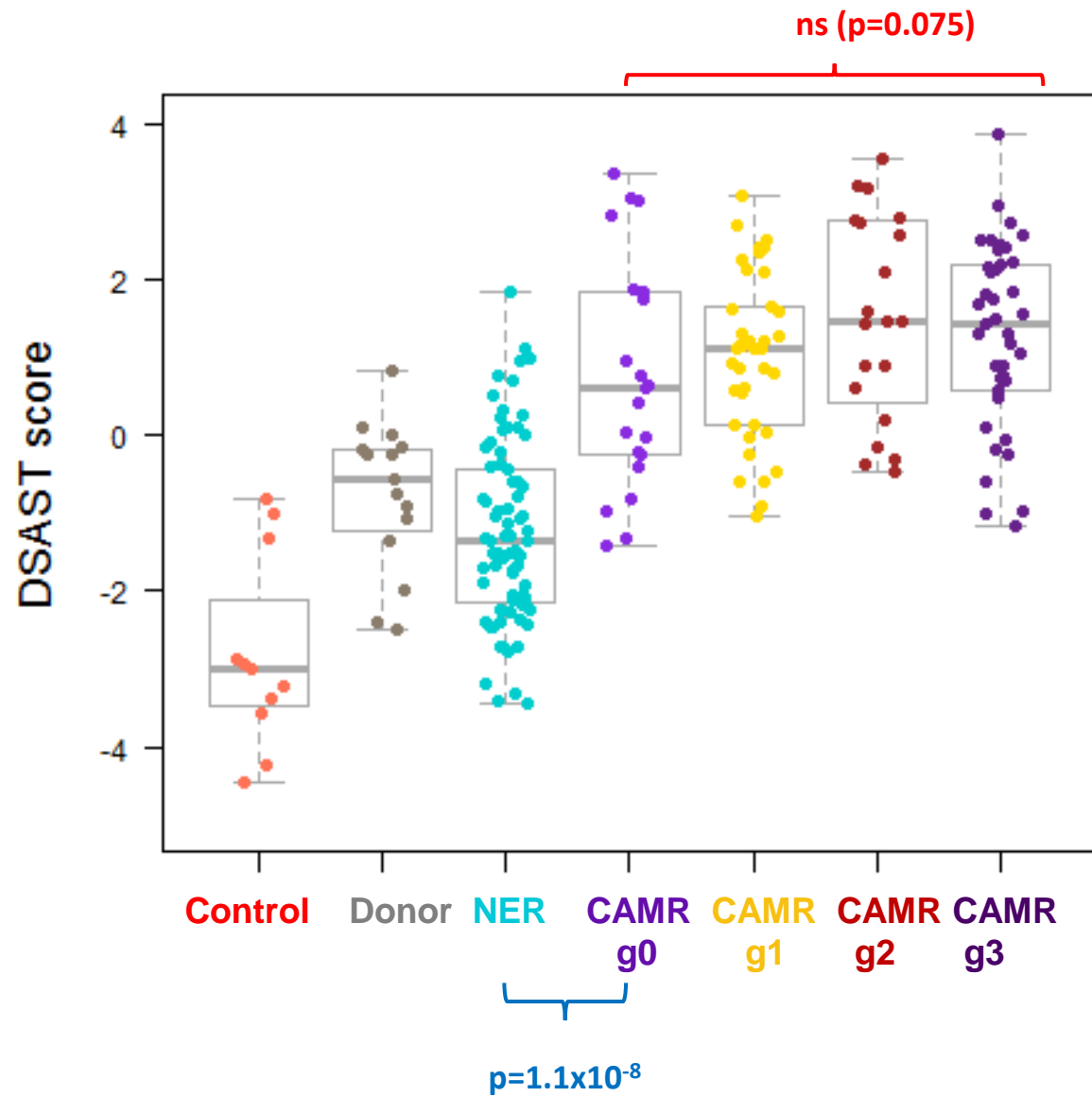
Supplemental Figure 4
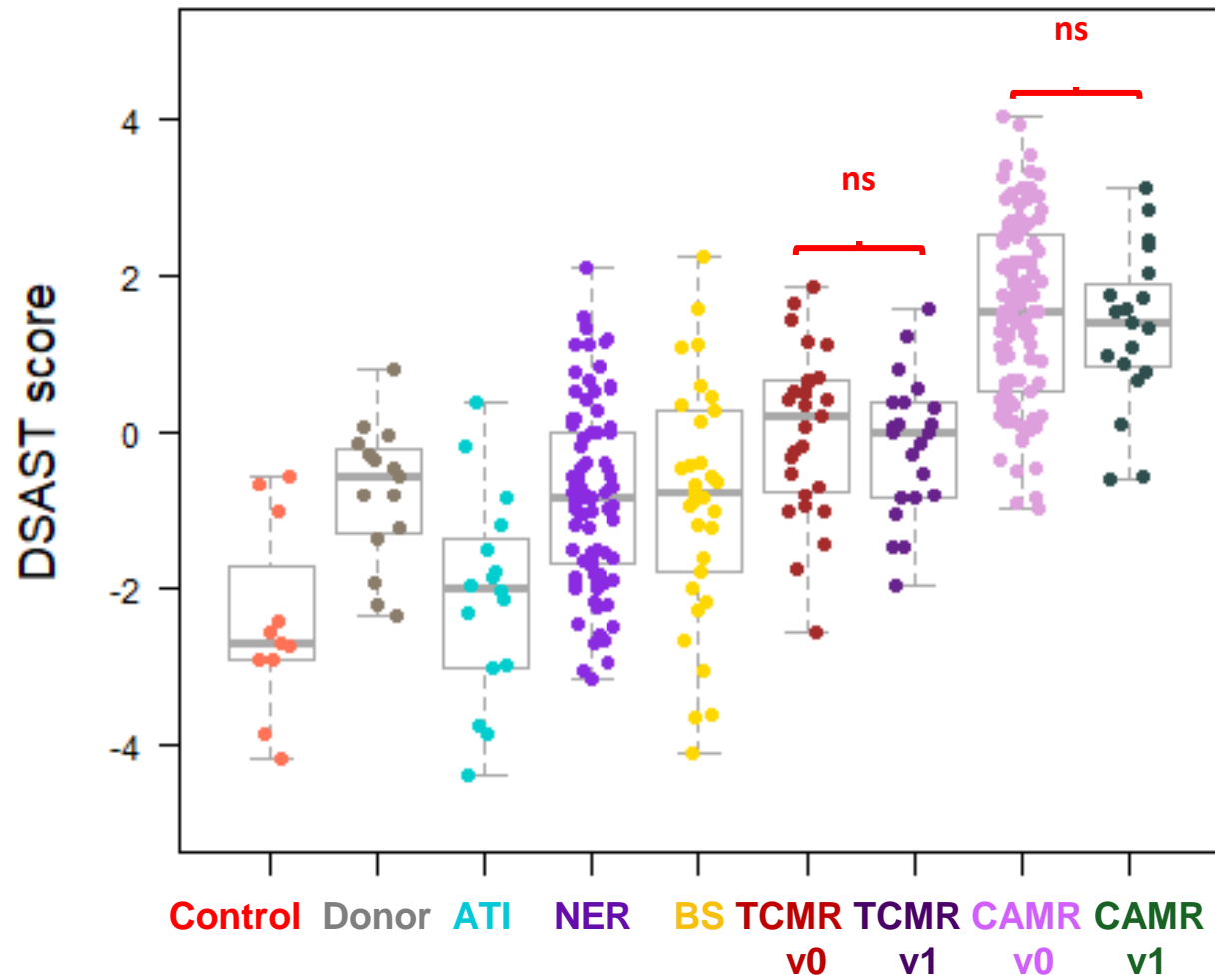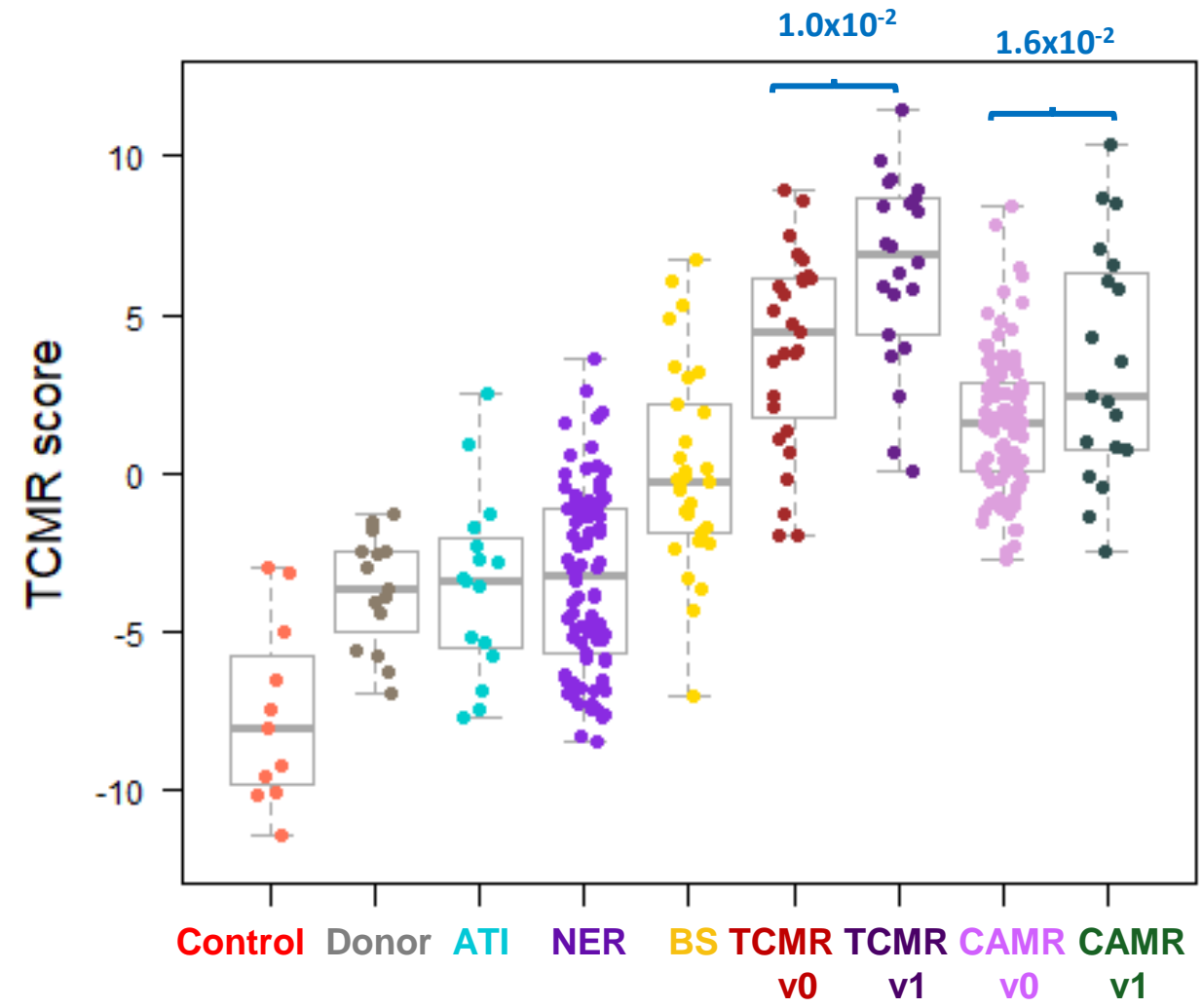
Supplemental Figure 5

Higher in DSA Neg

Gene	Log2 fold change	std error (log2)	BY.p.value
MET	-0.647	0.135	0.00393

Differential expression in DSA Pos CAMR vs baseline DSA Neg CAMR
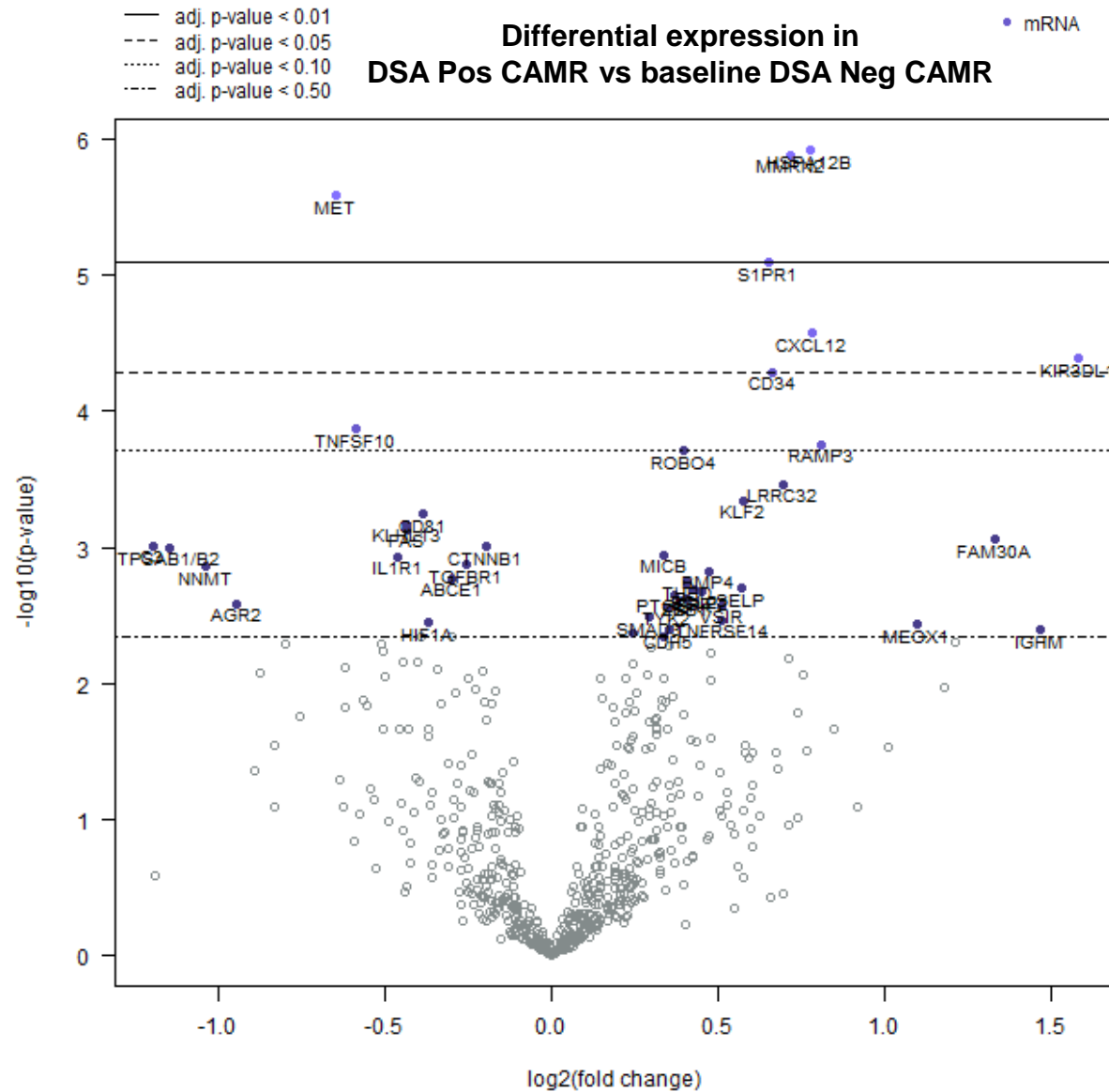
Higher in DSA Pos

Gene	Log2 fold change	std error (log2)	BY.p.value
KIR3DL1	1.58	0.377	0.0305
CXCL12	0.781	0.183	0.024
HSPA12B	0.777	0.156	0.00292
MMRN2	0.719	0.145	0.00292
CD34	0.662	0.161	0.0333
S1PR1	0.652	0.143	0.00912

Endothelial Genes

KIR3DL1 – NK cells
CXCL12 - chemotactic LC, angiogenesis

Supplemental Figure 6

A

M1 Gene panel

M1	
IL21R	IL12
CCL19	IL6
CCR7	LAG3
CD38	LILRB2
CD40	NOD1
CXCL10	PLA1A
CXCL13	SOCS1
CXCL9	TLR7
IDO1	TNF
	TNFAIP6

B

M2 Gene panel

M2
ALOX15
ARG1
CCL13
CCL18
CD163
CD68
CD209
IL10
MS4A6A
PDCD1LG2
TGFB1

Supplemental Figure 7

**Differential expression in
CAMR 3y graft failure vs baseline CAMR 3y surviving grafts**

CAMR excluding CAMR+TCMR
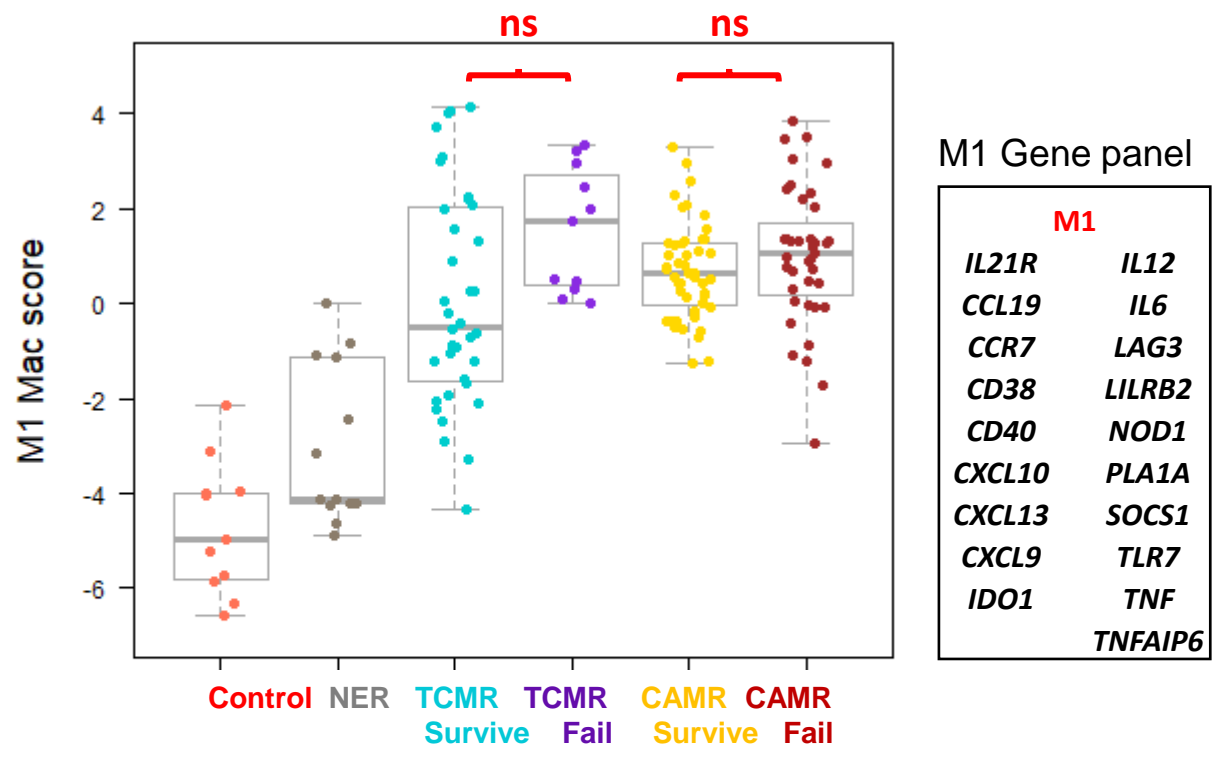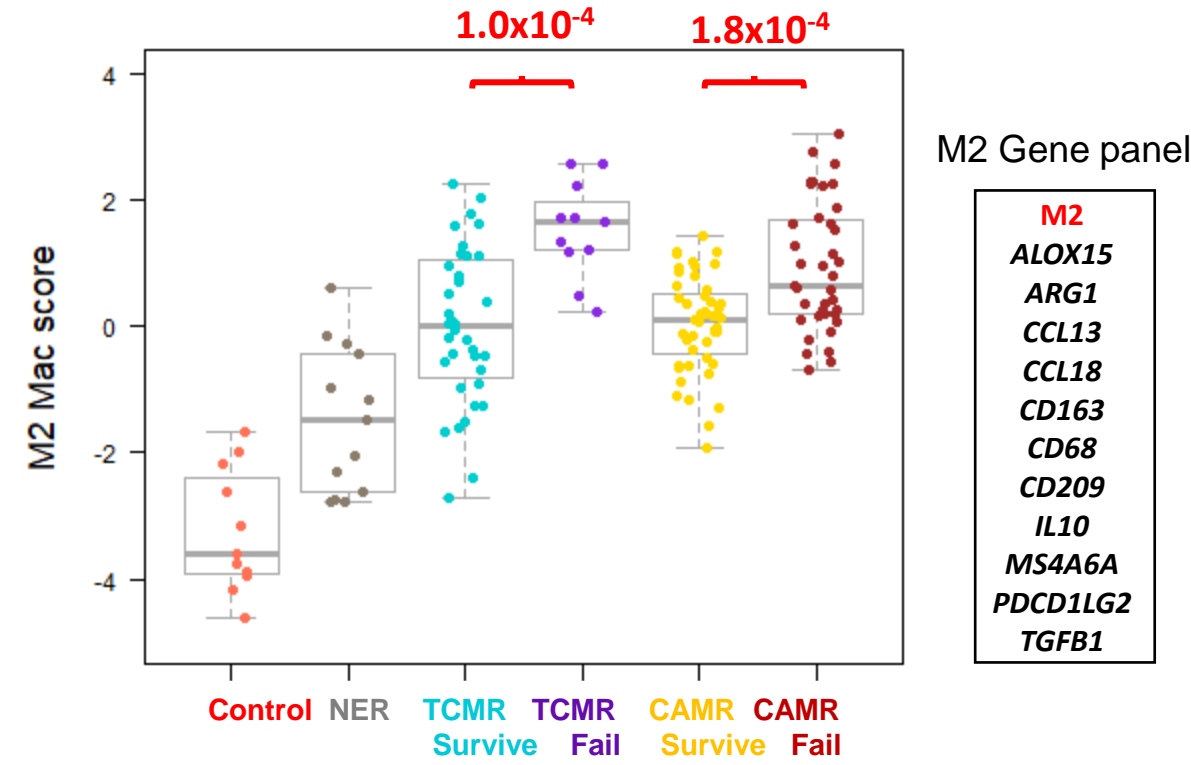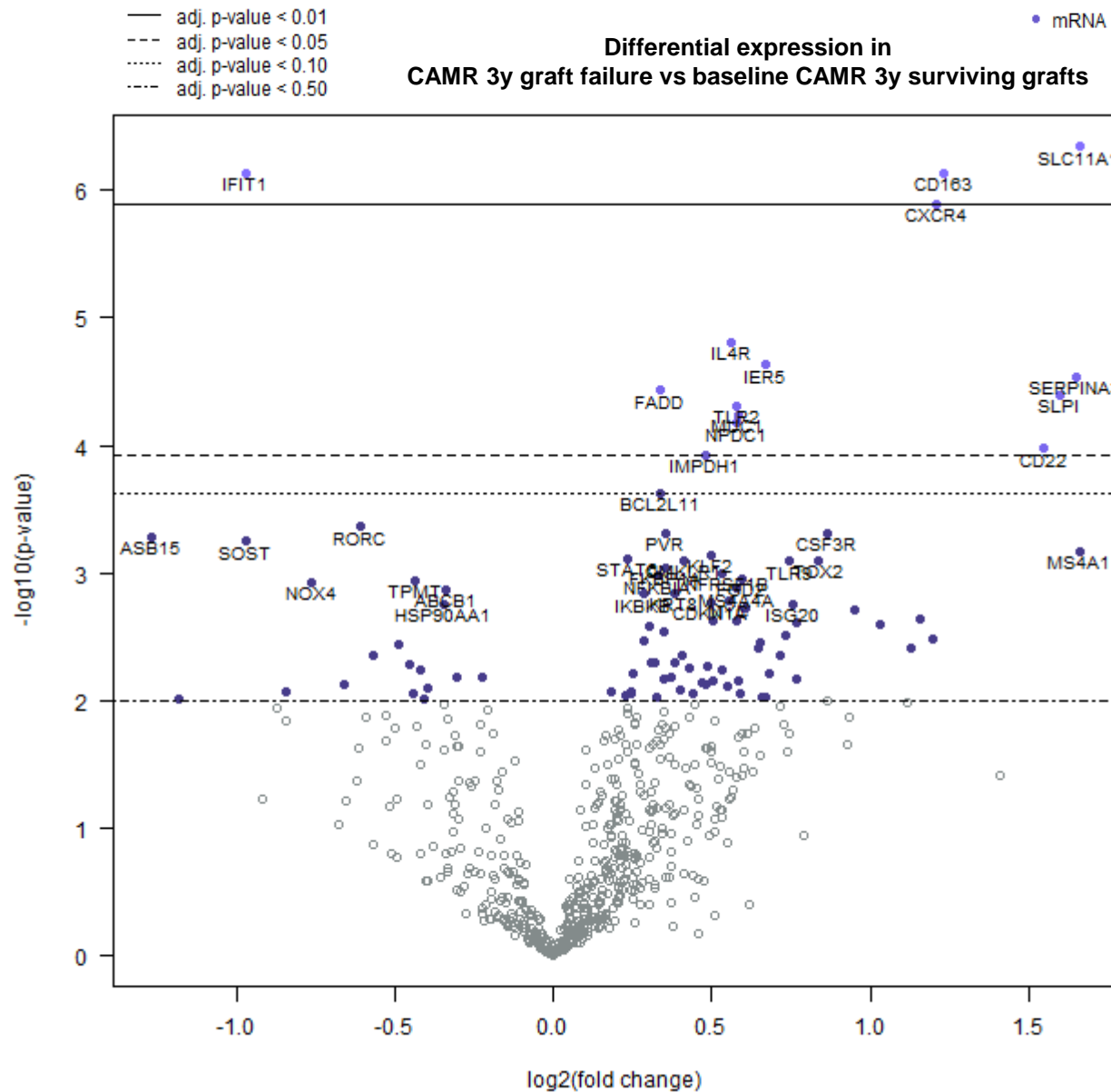
**CAMR
3 year graft failure**

Gene	Log2 fold change	std error (log2)	BY.p.value
SLC11A1	1.66	0.315	0.00112
SERPINA3	1.65	0.382	0.0191
SLPI	1.6	0.378	0.0207
CD22	1.55	0.389	0.0375
CD163	1.23	0.239	0.00112
CXCR4	1.21	0.24	0.00145
IER5	0.673	0.154	0.0178
MUC1	0.584	0.141	0.0243
NPDC1	0.58	0.141	0.0256
TLR2	0.576	0.138	0.0224
IL4R	0.559	0.125	0.0143
IMPDH1	0.479	0.121	0.0389
FADD	0.335	0.0788	0.0207

Macrophage

Supplemental Figure 8

BS-TCMR Survival

Gene	Log2 fold change	std error (log2)	BY.p.value
MME	-1.55	0.321	3.27E-03
ERRFI1	-1.38	0.363	2.92E-02
SLC22A2	-1.04	0.217	3.27E-03
ALDH3A2	-0.867	0.199	7.84E-03
AQP1	-0.777	0.196	1.85E-02
DCAF12	0.35	0.0784	5.95E-03
HLA-E	0.454	0.116	2.14E-02
FAS	0.56	0.139	1.68E-02
C5AR1	0.581	0.154	3.17E-02
BST2	0.594	0.146	1.68E-02
TLR4	0.633	0.127	3.27E-03
AXL	0.646	0.14	4.50E-03

Tubular Epithelium

BS-TCMR Fail

Gene	Log2 fold change	std error (log2)	BY.p.value
SLC11A1	1.61	0.411	2.14E-02
NNMT	1.46	0.391	3.32E-02
VWF	1.37	0.341	1.68E-02
CD163	1.3	0.327	1.79E-02
C1QB	1.23	0.299	1.53E-02
C1QA	1.15	0.268	8.64E-03
FN1	1.08	0.237	4.89E-03
MS4A4A	0.996	0.243	1.53E-02
FCGR2A	0.972	0.202	3.27E-03
FCER1G	0.961	0.246	2.14E-02
TLR2	0.93	0.184	3.27E-03

Macrophage

Endothelium

Differential expression in
BS-TCMR graft failure vs baseline BS-TCMR surviving grafts

Supplemental Figure 9
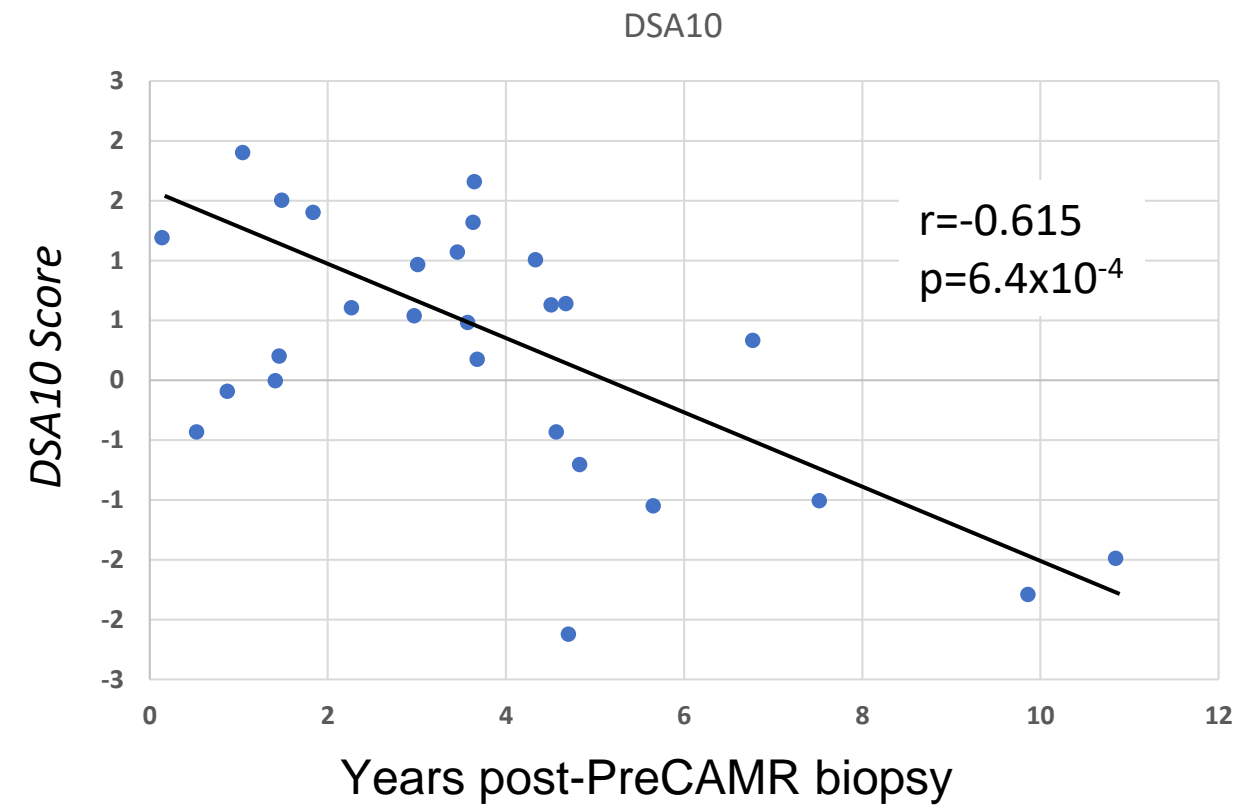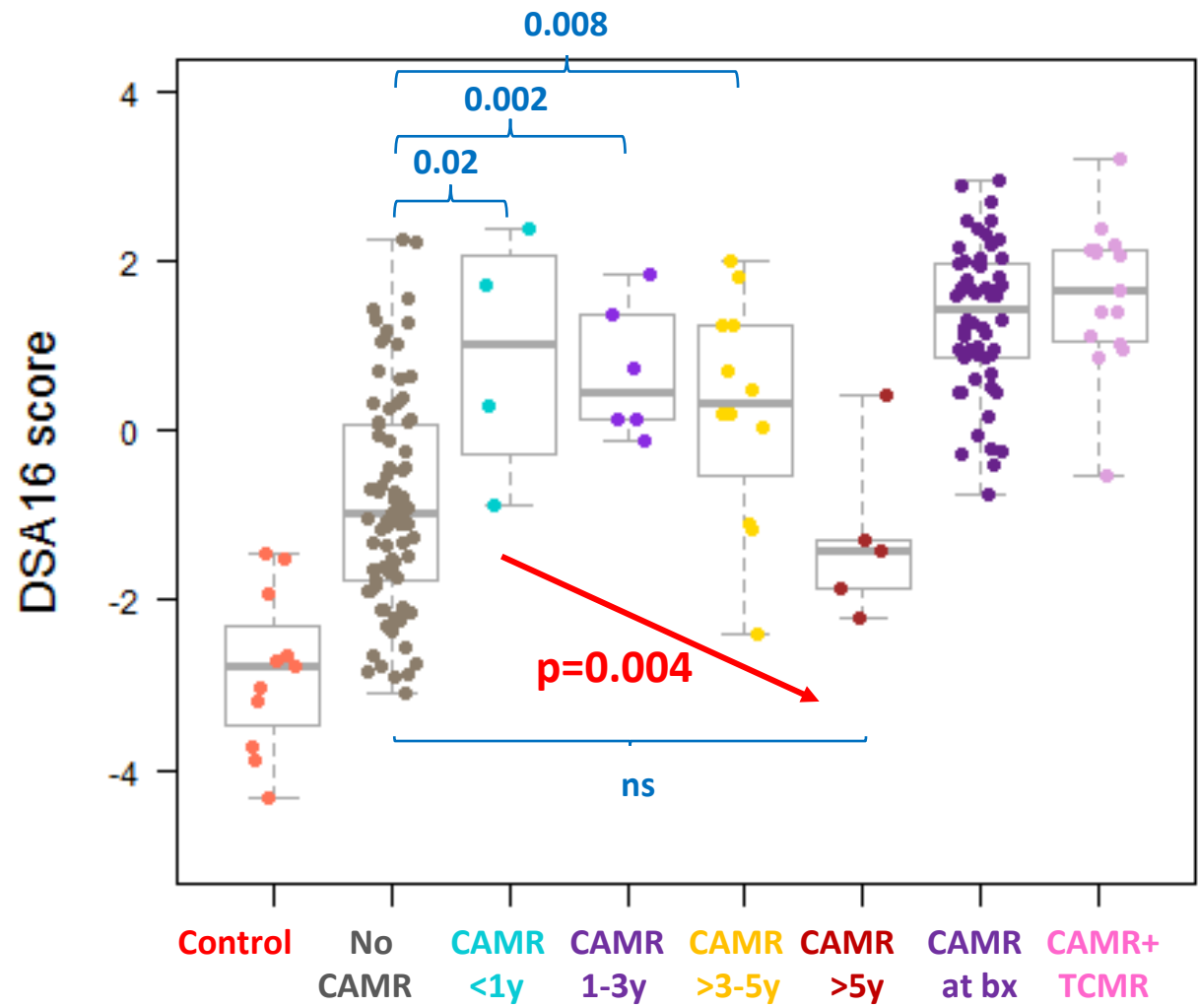
Supplemental Figure 10

Random Forest Outcome Classification

CAMR/Mixed

Confusion matrix (OOB sample):

RF Classification	Outcome Observed		Total	% Correct with RF Classification
	Survive	Fail		
Survive	42	11	53	79%
Fail	5	28	33	85%
Total	47	39	86	
% Correct without RF	55%	45%		

Chi2   6.4x10-9
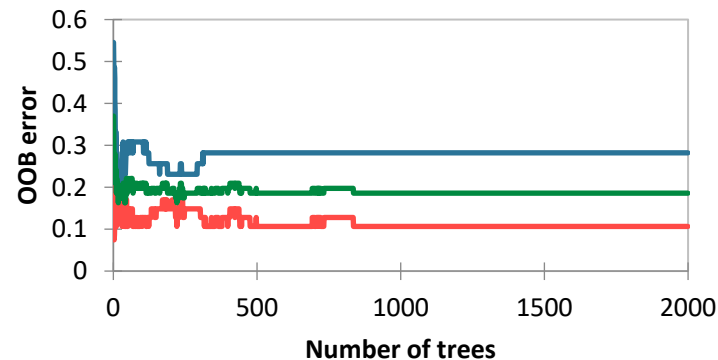
Forest type: Classification
Method: Bagging
Sampling method: Random with replacement
Sample sizes: 60
Required number of trees in the forest: 2000
Number of trees built: 2000
Seed (random numbers): 1757329514

OOB error evolution

(graph: OOB error vs Number of trees, x-axis 0 to 2000, y-axis 0 to 0.6)

Top 30 Variables by Importance

Variables	Overall
SLC11A1	36.879
Cr at biopsy	16.944
% Globally Sclerotic	16.150
CD207	13.359
CD163	11.187
Glomerular Endothelium	11.115
TLR2	10.249
IFIT1	9.740
CD274	9.533
NFKBIA	9.323
FCER1A	9.271
TNFRSF1B	8.700
ANKRD22	8.606
Complement Inhibition	7.464
CDKN1A	7.188
% C4d	7.135
MAPK13	6.574
PDGFRB	6.273
SERPINE1	6.243
SLC4A1	6.073
% i-IFTA	5.847
KT2	5.369
MRC1	5.268
ah	5.176
HLA-C	4.365
IL4R	3.354
i	3.238
ASB15	2.617
Years post transplant	2.597
Macrophages	2.428

Clinical/Lab
Pathway/Cell
Pathology
Gene

All higher in Fail group except KT2, Glomerular endothelium, FCER1A, ASB15, PDGFRB, IFIT1, CD207, SLC4A1

Supplemental Figure 11

Random Forest Outcome Classification

BS-TCMR

Confusion matrix
(OOB sample):

RF Classification	Outcome Observed		Total	% correct with RF Classification
	Survive	Fail		
Survive	37	5	42	88%
Fail	1	7	8	88%
Total	38	12	50	
% Correct without RF	76%	24%		
		Chi2	2.7x10-5	

Forest type: Classification
Method: Bagging
Sampling method: Random with replacement
Sample sizes: 35
Required number of trees in the forest: 2000
Number of trees built: 2000
Seed (random numbers): 671507506

OOB error evolution
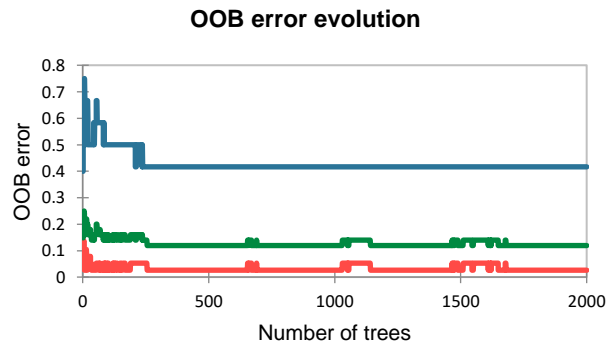
Top 39 Variables by Importance

Variables	Overall
Cytosolic DNA Sensing	12.491
Extracellular Matrix Organization	11.032
ALAS1	10.312
IFTA	10.246
TLR4	9.294
IFI6	8.973
Endothelium	8.932
CRIP2	8.635
CXCL16	8.605
CD14	8.211
Pan-BM	8.193
IRRAT	7.922
Years post transplantation	7.884
g	7.342
KRT8	6.930
M2 Macrophage	6.809
AKI	6.553
FAS	6.441
Fibrosis	6.035
Neutrophil degranulation	5.404
mi (ptc+g)	5.357
C1QA	5.345
NOS3	4.795
MS4A7	4.770
i	4.721
FCER1G	4.473
PLAUR	4.307
IRITD3	4.269
RHOJ	4.230
TLR5	4.211
DCAF12	3.061
COL3A1	2.836
ptc	2.781
Progression GoCAR	2.609
VWF	2.437
mTOR	2.356
MS4A6A	1.833
ITGAM	1.639
CCL21	0.835

Clinical/Lab

Pathway/Cell

Pathology

Gene

*All variables higher in Fail group, except i

Supplemental Figure 12A

CAMR/Mixed
Clinical and Lab Variables

Confusion matrix (OOB sample):

from \ to	G1 CAMR Survive	G2 CAMR Fail	Total	% correct
G1 CAMR Survive	37	7	44	84.1
G2 CAMR Fail	10	28	38	73.7
Total	47	35	82	79.3

Total Correct 79%

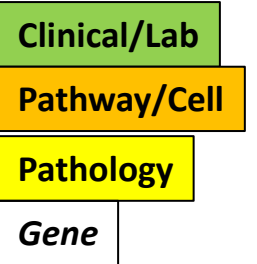| Variables	G1 CAMR Survive	G2 CAMR Fail	Overall
Cr at biopsy	62.480	70.302	80.164
Years post transplant	16.100	17.155	21.156
Age (yrs)	17.352	5.888	14.690
Gender	-2.184	10.105	7.200
# DSAs	-2.673	7.488	3.741
DSA	4.265	-0.492	2.282
Max MFI	-8.820	8.232	1.462
DSA Class	-2.293	-1.891	-2.838

Forest type: Classification
Method: Bagging

Sampling method: Random with replacement
Sample sizes: 70

Required number of trees in the forest: 2000

Number of trees built: 2000

Seed (random numbers): 692640582

OOB error evolution
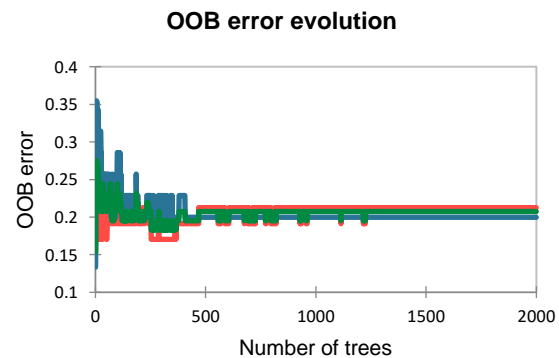
Omit 4 Cr>10

Supplemental Figure 12B

CAMR/Mixed
Pathology Variables

Confusion matrix (OOB sample):

from \ to	G1 CAMR Survive I	G2 CAMR Fail I	Total	% correct
G1 CAMR Survive	36	14	50	72.0
G2 CAMR Fail	11	25	36	69.4
Total	47	39	86	70.9

Total Correct 71%

Variables	G1 CAMR Survive	G2 CAMR Fail	Overall
%C4d	31.386	20.355	33.667
ah	17.586	18.760	24.310
i+t	13.034	13.561	17.326
i	8.461	9.734	12.081
C4d	12.066	1.597	10.369
% iIFTA	4.307	3.004	4.938
ci	-1.055	5.626	2.894
% fibrosis	2.351	1.782	2.856
% Globally Sclerotic	2.456	0.769	2.193
cv	-2.647	5.301	1.831
t	-1.718	3.313	1.282
v	-3.270	2.887	-0.044
cg	-3.386	1.863	-1.150
ct	-1.743	-0.036	-1.267
mi (ptc+g)	-7.455	5.160	-1.456
g	-3.818	1.038	-2.514
% tubular atrophy	-4.025	-2.417	-4.662
ptc	-5.832	-1.233	-4.777
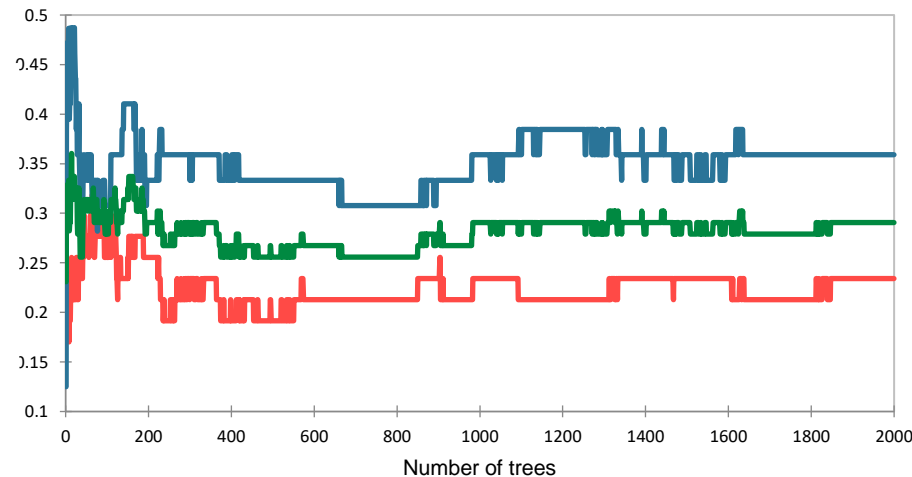
Forest type: Classification
Method: Bagging

Sampling method: Random with replacement
Sample sizes: 70
Required number of trees in the forest: 2000
Number of trees built: 2000

Seed (random numbers): 1110815619

OOB error evolution

Supplemental Figure 12C

CAMR/Mixed
Pathway/Cell Type Scores

Top 20

Confusion matrix (OOB sample):

| from \ to	G1 CAMR Survive I	G2 CAMR Fail I	Total	% correct
G1 CAMR Survive I	30	16	46	65.2
G2 CAMR Fail I	17	23	40	57.5
Total	47	39	86	61.6

Total Correct 62%

Forest type: Classification
Method: Bagging

Sampling method: Random with replacement
Sample sizes: 70

Required number of trees in the forest: 2000

Number of trees built: 2000

Seed (random numbers): 1362447273

OOB error evolution
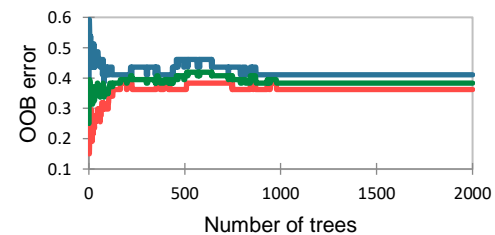
Variables	G1 CAMR Survive I	G2 CAMR Fail I	Overall
Complement Inhibition	17.871	16.179	21.304
KT2	9.924	9.046	12.058
Macrophages.vs.CD45	10.032	7.278	10.878
GBM	9.067	8.975	10.715
CD4.vs.CD45	7.846	7.330	9.322
Glomerular Endothelium	6.905	5.856	8.139
eGFR later	7.273	3.213	7.947
M2 Mac	7.714	3.842	7.728
AMAT1	5.305	5.309	7.558
MS1	3.466	6.983	7.368
Tubule	5.902	4.069	6.448
AKI	6.359	1.741	5.945
Rho GTPase signaling	3.227	4.872	5.486
Neutrophil degranulation	4.479	3.736	5.481
TGF-beta Signaling	3.290	2.439	4.261
KT1	0.330	5.362	4.235
Macrophages	3.176	3.496	4.132
M2 Mac10	5.323	-0.933	3.833
AMR	-0.030	4.803	3.613
IRRAT	3.084	0.357	3.454

Supplemental Figure 12D

CAMR/Mixed
Individual transcript counts

Confusion matrix (OOB sample):

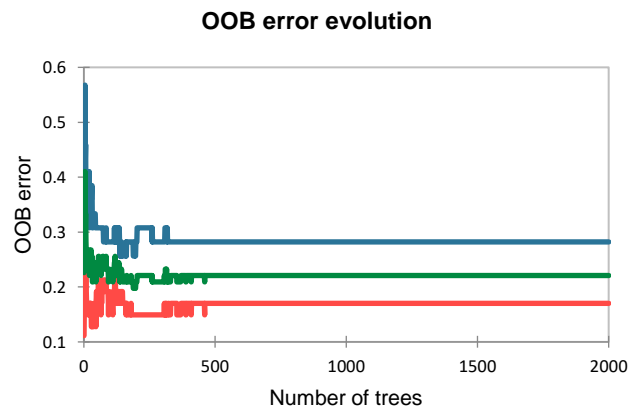| from \ to	G1 CAMR Survive I	G2 CAMR Fail I	Total	% correct
G1 CAMR Survive I	39	11	50	78.0
G2 CAMR Fail I	8	28	36	77.8
Total	47	39	86	77.9

Total Correct 78%

Forest type: Classification
Method: Bagging

Sampling method: Random with replacement
Sample sizes: 70

Required number of trees in the forest: 2000
Number of trees built: 2000

Seed (random numbers): 22568641

OOB error evolution

Top 25

Variables	G1 CAMR Survive I	G2 CAMR Fail I	Overall
SLC11A1	33.067	32.116	36.304
TLR2	9.610	10.232	11.251
CD274	-0.705	8.357	7.888
FCER1A	2.633	7.506	7.815
TNFRSF1B	7.231	5.093	7.308
CD163	6.628	5.328	7.082
NFKBIA	6.355	4.907	7.021
IFIT1	6.017	5.214	6.646
ANKRD22	3.034	6.481	6.369
SERPINE1	4.906	4.660	5.572
S100A9	4.038	4.490	5.168
SLC4A1	3.422	4.156	4.821
CD207	4.201	4.011	4.653
MALL	4.086	2.775	4.611
MRC1	3.506	3.015	3.950
MS4A4A	1.680	4.189	3.804
BRWD1	5.198	-1.134	3.749
CMKLR1	2.203	3.403	3.526
MAPK13	2.961	2.419	3.365
GBP5	-0.401	3.417	3.299
GIMAP5	1.655	2.393	3.245
TGIF1	3.214	2.391	3.208
CDH13	0.209	3.443	3.075
HYAL2	2.811	1.735	2.960
SLC12A3	3.036	1.070	2.887

Supplemental Figure 13A

BS-TCMR
Clin/Lab

Confusion matrix (OOB sample):

from \ to	F1 TCMR-BS Survive	F2 TCMR-BS Fail	Total	% correct
F1 TCMR-BS Survive	31	12	43	72.1
F2 TCMR-BS Fail	7	0	7	0.0
Total	38	12	50	62.0

Variables	F1 TCMR-BS Survive	F2 TCMR-BS Fail	Overall
DSA Present at biopsy 1-26-22	15.793	-3.273	12.383
# DSAs	2.131	-1.918	0.693
Years post tx (Calc)	3.479	-8.562	-2.162
Gender	-3.506	0.859	-2.482
Cr at time of bx	-4.201	-0.179	-2.953

Total Correct 62%

Forest type: Classification
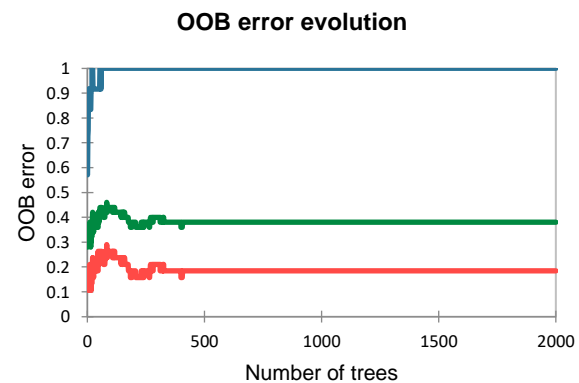Method: Bagging

Sampling method: Random with replacement
Sample sizes: 35

Required number of trees in the forest: 2000
Number of trees built: 2000

Seed (random numbers): 1975305146

OOB error evolution

Supplemental Figure 13B

Confusion matrix (OOB sample):

from \ to	F1 TCMR-BS Survive	F2 TCMR-BS Fail	Total	% correct
F1 TCMR-BS Survive	33	10	43	76.7
F2 TCMR-BS Fail	5	2	7	28.6
Total	38	12	50	70.0

BS-TCMR
Pathology

Variables	F1 TCMR-BS Survive	F2 TCMR-BS Fail	Overall
ptc	13.726	11.985	15.959
mi (ptc+g)	13.430	12.893	15.145
% fibrosis	11.399	9.040	12.930
g	11.801	5.629	10.765
C4d	9.980	4.232	8.763
% tubular atrophy	8.682	-3.054	5.962
i	11.635	-7.480	5.174
ct	4.102	-2.642	3.181
v	4.194	-2.874	2.525
t	4.979	-6.633	0.664

Total Correct 70%

Forest type: Classification
Method: Bagging

Sampling method: Random with replacement
Sample sizes: 35

Required number of trees in the forest: 2000
Number of trees built: 2000

Seed (random numbers): 678733136

OOB error evolution

Supplemental Figure 13C

Confusion matrix (OOB sample):

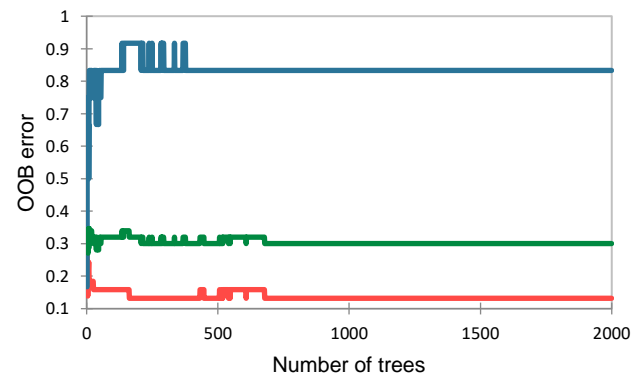| from \ to	F1 TCMR-BS Survive	F2 TCMR-BS Fail	Total	% correct
F1 TCMR-BS Survive	34	5	39	87.2
F2 TCMR-BS Fail	4	7	11	63.6
Total	38	12	50	82.0

Total Correct 82%

Forest type: Classification
Method: Bagging

Sampling method: Random with replacement
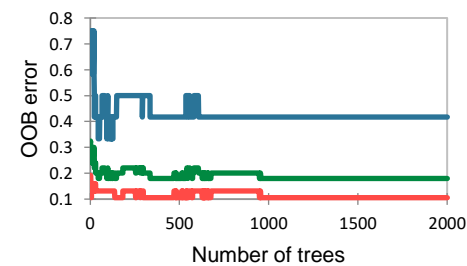Sample sizes: 35

Required number of trees in the forest: 2000

Number of trees built: 2000

Seed (random numbers): 651298721

OOB error evolution

BS-TCMR
Pathways/Cell Types

Variables	F1 TCMR-BS Survive	F2 TCMR-BS Fail	Overall
Extracellular Matrix Organization	17.438	9.663	16.878
Pan-BM	15.828	7.391	15.633
IRRAT	15.482	2.602	14.722
IFTA	7.710	6.094	8.830
Neutrophil degranulation	8.865	5.423	8.812
Endothelium	8.174	6.327	8.343
Macrophages	7.558	5.609	7.965
Cytosolic DNA Sensing	7.933	0.965	7.864
M2 Mac	6.785	4.650	7.081
IRITD5	5.690	4.292	6.033
Fibrosis	5.961	3.899	6.012
Complement Components	3.944	4.607	5.262
IRITD3	5.365	3.982	5.034
Complement Inhibition	3.676	3.558	4.853
AKI	6.453	1.416	4.679
KT1	2.625	4.132	4.187
NK	4.117	1.214	4.169
CAMR NHP	4.809	2.553	4.075
Progression GoCAR	3.953	1.820	3.583
ABMR-RATs	6.802	-2.633	3.347
M2 Mac11	2.933	1.967	3.057
Exhausted CD8	2.576	0.633	2.693
QCMAT	2.593	1.224	2.556
ENDAT	2.481	0.900	2.514
IL6 Signaling	2.310	0.426	2.482

Supplemental Figure 13D

BS-TCMR
Individual Transcripts

Confusion matrix (OOB sample):

from \ to	F1 TCMR-BS Survive	F2 TCMR-BS Fail	Total	% correct
F1 TCMR-BS Survive	33	9	42	78.6
F2 TCMR-BS Fail	5	3	8	37.5
Total	38	12	50	72.0

Total Correct 72%
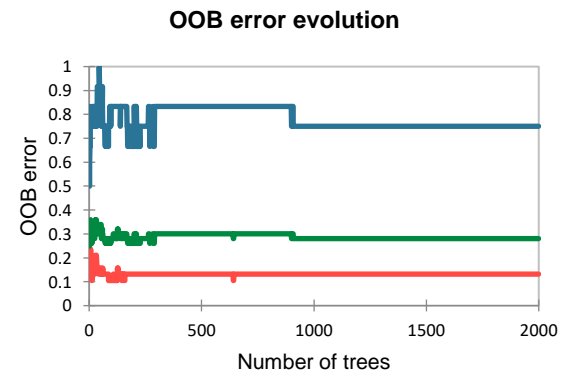
Forest type: Classification
Method: Bagging

Sampling method: Random with replacement
Sample sizes: 35

Required number of trees in the forest: 2000
Number of trees built: 2000

Seed (random numbers): 1908038177

OOB error evolution

Variables	F1 TCMR-BS Survive	F2 TCMR-BS Fail	Overall
FCGR2A	9.846	10.431	10.845
IFI6	8.048	7.693	8.259
KRT8	7.152	6.795	7.431
COL4A1	5.453	7.716	7.148
TLR4	5.963	5.227	6.251
FN1	4.919	6.165	5.992
CXCL16	4.644	5.303	5.358
CD14	4.288	4.896	5.024
CRIP2	4.401	4.181	4.415
ALAS1	3.857	4.356	4.253
ITGAX	4.025	2.548	4.099
FAS	3.725	3.889	4.091
MS4A7	3.199	4.178	3.932
COL1A1	3.042	3.654	3.831
C1QA	3.300	3.729	3.780
CD163	2.471	3.865	3.574
ITGB6	2.646	3.165	3.410
VWF	3.255	3.183	3.385
FCER1G	2.890	3.241	3.327
DCAF12	3.322	2.849	3.312
LCN2	3.278	3.129	3.288
TNF	3.022	1.029	3.243
RHOJ	2.865	2.872	3.028
ISG15	2.549	2.521	2.831
MS4A4A	2.051	2.790	2.736
AXL	2.460	2.447	2.620
PDCD1LG2	2.694	1.665	2.561
COL3A1	2.116	2.970	2.558
PLAUR	2.358	2.394	2.548
NOS3	2.371	2.351	2.514